Retention of Structural Cores in the Synthesis of High-Nuclearity Polyoxoalkoxomolybdate Clusters Encapsulating $[Na(H_2O)_3]^+$ and $[MoO_3]$ Moieties. Hydrothermal Syntheses and Structures of $(NH_4)_7[NaH_{12}Mo_{16}O_{52}]\cdot 4H_2O$ and $(Me_3NH)_4K_2[H_{14}Mo_{16}O_{52}]\cdot 8H_2O$ and Their Structural Relationships to the Class of Superclusters $[XH_nMo_{42}O_{109}\{(OCH_2)_3CR\}_7]^{m-}$ (X = $Na(H_2O)_3^+$: $n = 13$, $m = 9$; $n = 15$, $m = 7$. X = MoO_3: $n = 14$, $m = 9$; $n = 13$, $m = 10$)

M. Ishaque Khan,[†,‡] Qin Chen,[‡] Jose Salta,[‡] Charles J. O'Connor,[§] and Jon Zubieta*[,‡]

Departments of Chemistry, Syracuse University, Syracuse, New York 13244, and University of New Orleans, New Orleans, Louisiana 70148

Received July 13, 1995[⊗]

Hydrothermal reactions of molybdenum−oxide precursors with polyalcohols in the presence of base yielded two series of mixed-valence oxomolybdenum clusters, the hexadecanuclear species $[XH_{12}(Mo^{VI}O_3)_4Mo^{V}_{12}O_{40}]^{m-}$ (X = Na^+, $m = 7$; X = $2H^+$, $m = 6$) and the superclusters $[XH_nMo^{VI}_6Mo^{V}_{36}O_{109}\{(OCH_2)_3CR\}_7]^{m-}$ (X = $Na(H_2O)_3^+$, $m = 9$, $n = 13$; X = $Na(H_2O)_3^+$, $m = 7$, $n = 15$; X = MoO_3, $m = 9$, $n = 14$; X = MoO_3, $m = 10$, $n = 13$). In a representative synthesis for the hexadecanuclear class of materials, the hydrothermal reaction of a mixture of $Na_2MoO_4\cdot 2H_2O$, MoO_3, Mo metal, and NH_4Cl produced $(NH_4)_7[NaMo_{16}(OH)_{12}O_{40}]\cdot 4H_2O$ (**1**·$4H_2O$) as red-orange crystals. The compound $(Me_3NH)_4K_2[H_2Mo_{16}(OH)_{12}O_{40}]\cdot 8H_2O$ (**2**·$8H_2O$) was prepared in a similar fashion. The structure of the anion of **1** consists of an ϵ-Keggin core $\{H_{12}Mo_{12}O_{40}\}$, capped on four hexagonal faces by $\{MoO_3\}$ units and encapsulating a Na^+ cation. The structure of the oxomolybdenum framework of **2** is essentially identical to that of **1**; however, the central cavity is now occupied by $2H^+$. The synthesis of the "superclusters" exploits similar hydrothermal conditions, resulting in the isolation of $(Me_3NH)_2(Et_4N)Na_4[Na(H_2O)_3H_{15}Mo_{42}O_{109}\{(OCH_2)_3CCH_2OH\}_7]\cdot 15H_2O$ (**3**·$15H_2O$), $(Me_3NH)_2(H_3O)Na_6[Na(H_2O)_3H_{13}Mo_{42}O_{109}\{(OCH_2)_3CCH_2OH\}_7]\cdot 7H_2O$ (**4**·$7H_2O$), $Na_9[(MoO_3)H_{14}Mo_{42}O_{109}\{(OCH_2)_3CCH_2OH\}_7]\cdot 0.5C(CH_2OH)_4\cdot 25H_2O$ (**5**·$0.5C(CH_2OH)_4\cdot 25H_2O$), and $(Me_4N)(Et_2NH_2)(H_3O)_2Na_6$ $[(MoO_3)H_{13}Mo_{42}O_{109}\{(OCH_2)_3CCH_3\}_7]\cdot 10H_2O$ (**6**·$10H_2O$). The structures of these superclusters resemble a bowl consisting of an oxomolybdenum framework, constructed from eighteen pairs Mo(V)−Mo(V) dimers and linked through edge-sharing of $\{MoO_6\}$ octahedra, with six *cis*-dioxomolybdate(VI) sites protruding outward to provide the surface of a channel to the molecular cavity of the complex anion. The cavity is populated by a $Na(H_2O)_3^+$ group in **3** and **4** and by a $\{MoO_3\}$ unit in **5** and **6**. Crystal data are as follows. **1**·$4H_2O$: cubic $F\bar{4}3m$ (No. 216), $a = 26.978(3)$ Å, $Z = 8$. **2**·$8H_2O$: orthorhombic *Cmcm* (No. 63), $a = 18.493(4)$ Å, $b = 19.685(4)$ Å, $c = 19.518(4)$ Å, $Z = 4$. **3**·$15H_2O$: triclinic $P\bar{1}$ (No. 2), $a = 22.159(4)$ Å, $b = 27.049(5)$ Å, $c = 17.726(3)$ Å, $\alpha = 98.34(1)°$, $\beta = 112.56(2)°$, $\gamma = 82.81(1)°$, $Z = 2$. **4**·$7H_2O$: monoclinic $C2/c$ (No. 15), $a = 54.901(11)$ Å, $b = 17.616(4)$ Å, $c = 36.571(7)$ Å, $\beta = 94.04(2)°$, $Z = 8$. **5**·$0.5C(CH_2OH)_4\cdot 25H_2O$: triclinic $P\bar{1}$ (No. 2), $a = 17.302(3)$ Å, $b = 20.865(4)$ Å, $c = 26.734(5)$ Å, $\alpha = 103.90(3)°$, $\beta = 99.26(3)°$, $\gamma = 108.95(3)°$, $Z = 2$. **6**·$10H_2O$: orthorhombic *Pbcm* (No. 57), $a = 17.916(4)$ Å, $b = 44.614(9)$ Å, $c = 23.472(5)$ Å, $Z = 4$.

The synthesis of high-nuclearity cluster molecules with dimensions in the mesoscopic or nanometer size range is a challenge which has attracted increased attention in the design of materials of complexity intermediate to molecular compounds and infinite arrays of solid phase materials.[1−4] The metal chalcogenides, most notably the non-sulfur clusters, represent one example of molecules derived from the aggregation of fundamental building blocks into a variety of complex structures of varied properties.[5,6] The polyoxoanions[7−9] provide another class of soluble clusters whose structures can be expanded by further aggregation.[10] Thus, substitution of less positive metal centers, such as V(IV) units, into the Mo(VI) α-Keggin core, $[Mo_{12}AsO_{40}]^{3-}$, results in highly negatively charged and nucleophilic intermediates, such as $[Mo_8V_4AsO_{40}]^{11-}$,[10] which can then be linked to cationic moieties to produce superclusters.

The reactivity of related highly charged polyoxomolybdate clusters may be combined with the stability afforded metal oxide aggregates by the replacement of oxo groups by alkoxide ligands, and with the concomitant reduction of negative charge, to give polyoxoalkoxometalate moieties of general composition $[M_xO_y(OR)_z]^n$, where n may be, at least conceptually, positive.

[†] Current address: Department of Chemical and Biological Sciences, Illinois Institute of Technology, Chicago, IL 60616.
[‡] Syracuse University.
[§] University of New Orleans.
[⊗] Abstract published in *Advance ACS Abstracts,* February 15, 1996.

(1) DiSalvo, F. J. *Science* **1990**, *247*, 690.
(2) Lindsey, J. S. *New J. Chem.* **1991**, *15*, 153.
(3) Teo, B. K.; Zhang, H. *Angew. Chem., Int. Ed. Engl.* **1992**, *31*, 445 and references therein.
(4) Schmid, G. *Polyhedron* **1988**, *7*, 2321.
(5) You, J.-F.; Papaefthymiou, G. C.; Holm, R. H. *J. Am. Chem. Soc.* **1992**, *114*, 2692 and references therein.
(6) You, J.-F.; Snyder, B. S.; Papaefthymiou, G. C.; Holm, R. H. *J. Am. Chem. Soc.* **1990**, *112*, 1067.
(7) For a recent review of the scope of these materials see: Pope, M. T., Müller, A., Eds. *Polyoxometalates from Platonic Solids to Anti-Retroviral Activity*; Kluwer Academic Publishers: Dordrecht, The Netherlands, 1994.
(8) Pope, M. T.; Müller, A. *Angew. Chem., Int. Ed. Eng.* **1991**, *30*, 34.
(9) Pope, M. T. *Heteropoly and Isopoly Oxometalates*; Springer Verlag: New York, 1983.
(10) Müller, A.; Plass, W.; Krickemeyer, E.; Dillinger, S.; Bögge, H.; Armatage, A.; Proust, A.; Beugholt, C.; Bergmann, U. *Angew. Chem., Int. Ed. Engl.* **1994**, *33*, 849.

0020-1669/96/1335-1880$12.00/0

Scheme 1

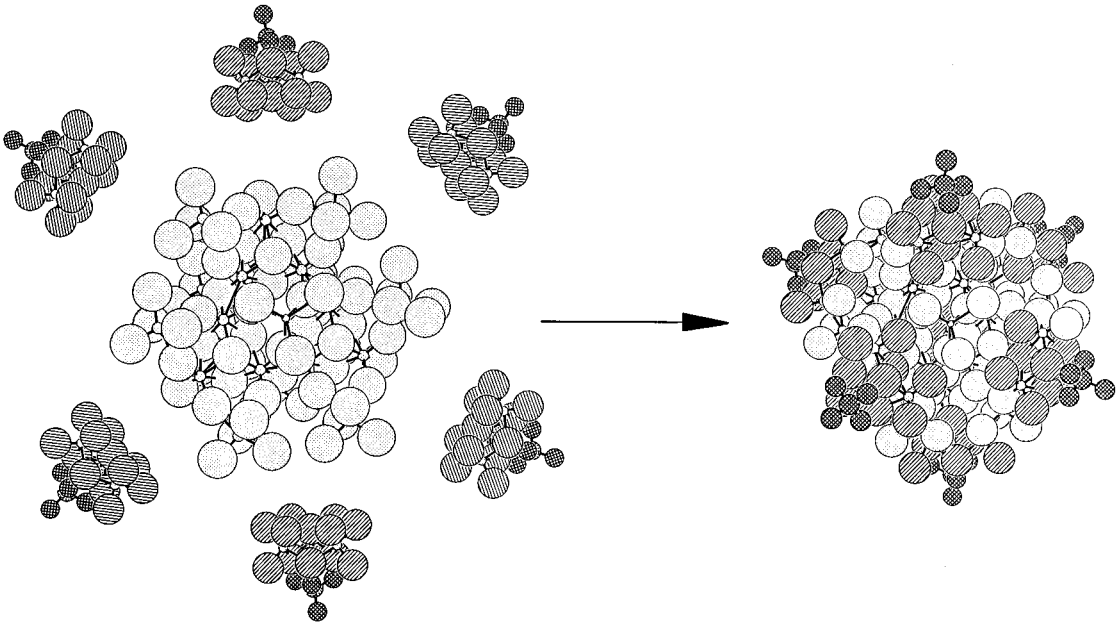

While polyoxoalkoxometalate cluster chemistry remains relatively undeveloped,[11] the occurrence of "oxidized" clusters, such as $[Ti_7O_4(OEt)_{20}]$[12] and $[Nb_8O_{10}(OEt)_{20}]$,[13] as well as "reduced" and mixed-valence polynuclear cores, represented by $[V_{16}O_{20}\{(OCH_2)_3CCH_2OH\}_8(H_2O)_4]$[14] and $[V_6O_9(OH)_4\{(OCH_2)_3CCH_3\}_2]^{2-}$,[15] respectively, establishes these clusters as a class of materials of unusual structural and electronic variety. In the course of our studies of the coordination chemistry of polyoxometalates with alkoxide ligands,[16] we have noted that tris(alkoxy) ligands of the class $(HOCH_2)_3CR$ are particularly effective in stabilizing triangular cluster fragments $\{M_3O_n(OCH_2)_3CR\}$, which may in turn aggregate to form higher nuclearity assemblages. Since the charge reduction afforded by the incorporation of the alkoxide ligand into the polyoxoalkoxometalate moiety can result in cationic fragments, it should be possible to link these to a highly negatively charged polyoxometalate cores to produce the supercluster, as shown in Scheme 1.

While the ability to synthesize high-nuclearity inorganic clusters according to rational design is still somewhat primitive, a combination of strategies is available for the construction of complex molecular assemblies. Although the fragment condensation process outlined above provides a satisfactory conceptual framework for the preparation of tailor-made clusters by control of inorganic hydrolysis−condensation and aggregation reactions, structural preassembly of such fragments in fact relies on "self-assembly" from simple soluble precursors. A significant expansion of exploitable building blocks may be achieved by adopting the techniques of hydrothermal synthesis.[17−19] When the reactions are carried out in water at 150−250 °C under autogenous pressure, the viscosity of water is lowered, resulting in enhanced rates of solvent extraction of solids and of crystal growth from solution.[19] Since differential solubility problems are minimized, a variety of synthetic precursors may be introduced. An additional advantage is that a variety of templating species may be employed and, during the crystallization process, the templates of appropriate size or geometry to fill the crystal vacancies or to drive the organization of cluster framework[20] are "selected" from the mixture. It is noteworthy that high-nuclearity polyoxoalkoxometalates such as $[Mg_2Mo_8O_{22}(OR)_6(HOR)_4]^{2-}$ [21] possess cavities for the incorporation of electropositive groups, in a manner reminiscent of the encapsulation of guest molecules in classical host−guest chemistry.[22,23]

The synthesis of the superclusters of general composition $[H_nMo_{42}O_{109}\{(OCH_2)_3CR\}_7]^{(23-n)-}$ [24] appears to rely upon an appropriate combination of these synthetic strategies. The formation of the structural core $[H_nMo_{16}O_{52}]^{(20-n)-}$ [25] relies on "self-assembly" under hydrothermal and reducing conditions. The modular design of the supercluster requires condensation of the constituent units of appropriate geometry and composition into the larger framework. Furthermore, detailed synthetic studies have established the necessity of introducing appropriate templates to effect organization of the framework. In this report, we describe the synthesis and structures of the mixed-valence Mo(V)/Mo(VI) polyanion clusters with a central ϵ-Keggin structure $(NH_4)_7[NaMo_{16}(OH)_{12}O_{40}]\cdot 4H_2O$ (**1**·$4H_2O$) and $(Me_3NH)_4K_2[H_2Mo_{16}(OH)_{12}O_{40}]\cdot 8H_2O$ (**2**·$8H_2O$), whose topological relationship to the superclusters reveals an underlying chemical relationship.[26] The structural systematics of the family of superclusters $(Me_3NH)_2(Et_4N)Na_4[Na(H_2O)_3H_{15}Mo_{42}O_{109}$-

(11) Chen, Q.; Zubieta, J. *Coord. Chem. Rev.* **1992**, *114*, 107.
(12) Day, V. W.; Eberspecher, T. A.; Klemperer, W. G.; Park, C. W.; Rosenberg, F. S. *J. Am. Chem. Soc.* **1991**, *113*, 8190. Watenpaugh, K.; Caughlan, C. N. *J. Chem. Soc., Chem. Commun.* **1967**, 76.
(13) Bradley, D. C.; Hursthouse, M. B.; Rodisila, P. F. *J. Chem. Soc., Chem. Commun.* **1968**, 1112.
(14) Khan, M. I.; Lee, Y.-S.; O'Connor, C. J.; Zubieta, J. *J. Am. Chem. Soc.* **1994**, *116*, 5001.
(15) Khan, M. I.; Chen, Q.; Goshorn, D. P.; Zubieta, J. *Inorg. Chem.* **1993**, *32*, 672. Khan, M. I.; Chen, Q.; Goshorn, D. P.; Höpe, H.; Parkin, S.; Zubieta, J. *J. Am. Chem. Soc.* **1992**, *114*, 3341.
(16) Zubieta, J. *Mol. Eng.* **1993**, *3*, 93 and references therein.
(17) Figlarz, M. *Chem. Scr.* **1988**, *28*, 3.
(18) Rouxel, J. *Chem. Scr.* **1988**, *28*, 33. Livage, J. *Chem. Scr.* **1988**, *28*, 9.
(19) Laudise, R. A. *Chem. Eng. New* **1987** (Sept. 28), 30.
(20) Reuter, H. *Angew. Chem., Int. Ed. Engl.* **1992**, *31*, 1185.
(21) Antipas, M. Yu.; Didenko, L. P.; Kachapina, L. M.; Shilov, A. G.; Shilova, A. K.; Struchkov, Y. T. *J. Chem. Soc., Chem. Commun.* **1989**, 1467.
(22) Klemperer, W. G.; Marquart, T. A.; Yaghi, O. M. *Angew. Chem., Int. Ed. Engl.* **1992**, *31*, 49 and references therein.
(23) Yang, X.; Knobler, C. B.; Hawthorne, M. F. *J. Am. Chem. Soc.* **1993**, *115*, 4904 and references therein.
(24) Khan, M. I.; Zubieta, J. *J. Am. Chem. Soc.* **1992**, *114*, 10058.
(25) Khan, M. I.; Müller, G.; Dillinger, S.; Bögge; H.; Chen, Q.; Zubieta, J. *Angew. Chem., Int. Ed. Engl.* **1993**, *32*, 1780.

Table 1. Crystallographic Data for the Structural Studies of $(NH_4)_7[NaMo_{16}(OH)_{12}O_{40}]\cdot 4H_2O$ (**1**·$4H_2O$), $(Me_3NH)_4K_2[H_2Mo_{16}(OH)_{12}O_{40}]\cdot 8H_2O$ (**2**·$8H_2O$), $(Me_3NH)_2(Et_4N)Na_4[Na(H_2O)_3H_{15}Mo_{42}O_{109}\{(OCH_2)_3CCH_2OH\}_7]\cdot 15H_2O$ (**3**·$15H_2O$), $(Me_3NH)_2(H_3O)Na_6[Na(H_2O)_3H_{13}Mo_{42}O_{109}\{(OCH_2)_3CCH_2OH\}_7]\cdot 7H_2O$ (**4**·$7H_2O$), $Na_9[(MoO_3)H_{14}Mo_{42}O_{109}\{(OCH_2)_3CCH_2OH\}_7]\cdot 0.5C(CH_2OH)_4\cdot 25H_2O$ (**5**·$0.5C(CH_2CH)_4\cdot 25H_2O$), $(Me_4N)(Et_2NH_2)(H_3O)_2Na_6[(MoO_3)H_{13}Mo_{42}O_{109}\{(OCH_2)_3CCH_3\}_7]\cdot 10H_2O$ (**6**·$10H_2O$)

	1·$4H_2O$	**2**·$8H_2O$	**3**·$15H_2O$	**4**·$7H_2O$	**5**·$0.5C(CH_2OH)_4\cdot 25H_2O$	**6**·$10H_2O$
empirical formula	$H_{48}N_7O_{56}NaMo_{16}$	$C_{12}H_{70}N_4O_{60}K_2Mo_{16}$	$C_{49}H_{154}N_3Na_5O_{155}Mo_{42}$	$C_{41}H_{119}N_2Na_7O_{148}Mo_{42}$	$C_{37.5}H_{133}O_{167}Na_9Mo_{43}Na_6O_{145}Mo_{43}$	$C_{43}H_{126}N_2Na_6O_{145}Mo_{43}$
a, Å	26.978(3)	18.493(4)	22.159(4)	54.901(11)	17.302(3)	17.916(4)
b, Å		19.685(4)	27.049(5)	17.616(4)	20.865(4)	44.614(9)
c, Å		19.518(4)	17.726(3)	36.571(7)	26.734(5)	23.472(5)
α, deg			98.34(1)		103.90(3)	
β, deg			112.56(2)	94.04(2)	99.26(3)	
γ, deg			82.81(1)		108.95(3)	
V, Å^3	19539(10)	7105(4)	9680(3)	35281(13)	8555(4)	18761(7)
Z	8	4	2	8	2	4
fw	2600.5	2843.9	7410.2	7199.0	7587.4	7254.9
space group (No.)	*F*$\bar{4}$3*m* (216)	*Cmcm* (63)	*P*$\bar{1}$ (2)	*C*2/*c* (15)	*P*$\bar{1}$ (2)	*Pbcm* (57)
T, °C	−60	21	−60	−153	−60	21
λ, Å	0.710 73	0.710 73	0.710 73	1.541 78	0.710 73	0.710 73
D_{calc}, g cm^{-3}	1.768	2.658	2.542	2.710	2.945	2.568
μ, cm^{-1}	20.50	26.58	27.10	247.80	31.74	28.79
R^a	0.0762	0.0477	0.0638	0.0653	0.0790	0.0621
$R_w{}^b$	0.0944	0.0526	0.0696	0.0755	0.0967	0.0705

[a] $\sum ||F_o| - |F_c||/\sum |F_o|$. [b] $[\sum w(|F_o| - |F_c|)^2/\sum w|F_o|^2]^{1/2}$.

Table 2. Atomic Positional Parameters ($\times 10^4$) and Isotropic Temperature Factors (Å^2 $\times$ 10^3) for $(NH_4)_7[NaMo_{16}(OH)_{12}O_{40}]\cdot 4H_2O$ (**1**·$4H_2O$)

	x	*y*	*z*	*U*(eq)[a]
Mo(1)	8726(1)	2154(3)	2840(2)	24(1)
Mo(2)	1549(1)	1549(1)	1549(1)	25(1)
Na	7500	2500	2500	54(7)
O(1)	9341(7)	2114(33)	2959(33)	28(5)
O(2)	8131(6)	1191(13)	1120(13)	28(6)
O(3)	8612(6)	2085(12)	2152(13)	21(6)
O(4)	8613(13)	2136(7)	3627(13)	31(6)
O(5)	2966(6)	2966(6)	2966(6)	16(6)
O(6)	0	0	919(42)	80(33)
O(7)	5000	1604	1558(56)	114(39)
N(1)	0	1892(14)	1892(14)	45(14)
N(2)	5000	0	1970(23)	70(19)

[a] Equivalent isotropic *U* defined as one-third of the trace of the orthogonalized $\mathbf{U}_{ij}$ tensor.

Table 3. Atomic Positional Parameters ($\times 10^4$) and Isotropic Temperature Factors (Å^2 $\times$ 10^3) for $(Me_3NH)_4K_2[H_2Mo_{16}(OH)_{12}O_{40}]\cdot 8H_2O$ (**2**·$8H_2O$)

	x	*y*	*z*	*U*(eq)[a]
Mo(1)	0	4224(1)	6836(1)	27(1)
Mo(2)	703(1)	873(1)	7500	26(1)
Mo(3)	1611(1)	2081(1)	6641(1)	26(1)
Mo(4)	912(1)	3013(1)	5975(1)	26(1)
Mo(5)	0	1230(1)	5664(1)	27(1)
Mo(6)	1969(1)	3850(1)	7500	30(1)
K(1)	2168(4)	4332(4)	2500	117(4)
O(1)	784(6)	4066(5)	7500	25(3)
O(2)	1546(4)	3065(4)	6785(4)	29(2)
O(3)	937(6)	1927(6)	7500	29(3)
O(4)	0	1039(6)	8246(5)	28(3)
O(5)	752(4)	2033(4)	6046(3)	25(2)
O(6)	0	3167(6)	6629(6)	30(3)
O(7)	0	3021(6)	5321(5)	28(3)
O(8)	2303(6)	2065(6)	7500	29(3)
O(9)	1519(4)	1007(4)	8248(4)	31(2)
O(10)	0	5069(7)	6697(6)	39(4)
O(11)	844(7)	37(6)	7500	35(4)
O(12)	794(4)	4074(4)	6078(4)	33(3)
O(13)	0	1701(6)	10108(5)	31(4)
O(14)	2781(7)	3404(7)	7500	38(4)
O(15)	2322(4)	1966(4)	6104(4)	36(3)
O(16)	750(5)	705(4)	9416(4)	37(3)
O(17)	2028(4)	4396(4)	8203(4)	35(3)
O(18)	1465(5)	3115(4)	5295(4)	36(3)
O(19)	4525(12)	815(11)	9510(12)	65(6)
O(20)	3541(21)	1066(19)	8744(20)	139(13)
O(21)	4241(27)	1238(24)	7500	116(16)
N(1)	1192(15)	1534(14)	907(14)	59(7)
N(2)	1517(16)	1044(14)	567(15)	65(8)
C(1)	1134(9)	845(8)	1235(9)	60(4)
C(2)	1855(11)	1672(10)	571(10)	79(6)
C(3)	1077(21)	2103(19)	1332(19)	74(10)
C(4)	2067(23)	600(21)	329(21)	85(12)

[a] Equivalent isotropic *U* defined as one-third of the trace of the orthogonalized $\mathbf{U}_{ij}$ tensor.

$\{(OCH_2)_3CCH_2OH\}_7]\cdot 15H_2O$ (**3**·$15H_2O$), $(Me_3NH)_2(H_3O)Na_6[Na(H_2O)_3H_{13}Mo_{42}O_{109}\{(OCH_2)_3CCH_2OH\}_7]\cdot 7H_2O$ (**4**·$7H_2O$), $Na_9[(MoO_3)H_{14}Mo_{42}O_{109}\{(OCH_2)_3CCH_2OH\}_7]\cdot 0.5C(CH_2OH)_4\cdot 25H_2O$ (**5**·$0.5C(CH_2OH)_4\cdot 25H_2O$), and $(Me_4N)(Et_2NH_2)(H_3O)_2Na_6[(MoO_3)H_{13}Mo_{42}O_{109}\{(OCH_2)_3CCH_3\}_7]\cdot 10H_2O$ (**6**·$10H_2O$) are discussed, as well as the syntheses directly from simple synthetic precursors and from **1** and **2**.

Experimental Section

Reagent grade chemicals were used throughout. Molybdenum metal (−325 mesh, Cerac), K_2MoO_4 (Aldrich), $Na_2MoO_4\cdot 2H_2O$ (Aldrich), MoO_3 (Aldrich), 1,1,1-tris(hydroxymethyl)alkanes (Aldrich), pentaerythritol (Aldrich), tetraethylammonium chloride (Aldrich), and various alkylamines (Aldrich) were used as received from the commercial sources. All reactions were carried out in 23 mL Parr Teflon-lined acid digestion bombs, heated in a Thermolyne programmable electric furnace. While preparations using each of the ligand types $RC(CH_2OH)_3$ (R = $-CH_3$, $-CH_2CH_3$, $-CH_2OH$) were attempted for all sets of conditions, synthetic details are given only for those instances which produced monophasic crystalline materials in appreciable yield.

$(NH_4)_7[NaMo_{16}(OH)_{12}O_{40}]\cdot 4H_2O$ (1·$4H_2O$). Method A. A mixture of $Na_2MoO_4\cdot 2H_2O$, MoO_3, Mo (−325 mesh), $(OHCH_2)_4C$, Me_3NHCl, Et_4NCl, and H_2O in the mole ratio 6:6:4:10:10:10:300 was placed in a 23 mL Teflon-lined autoclave which was subsequently heated for 3 days inside an electric furnace maintained at 160 °C. After the autoclave was cooled to room temperature over a period of 3−4 h, dark red-brown crystals of **3**·$15H_2O$ were filtered from the red-brown filtrate. Upon standing for 10 days at room temperature, the filtrate deposited red-orange cubic crystals of **1**·$4H_2O$. Since the crystals of **1**·$4H_2O$ turn opaque upon exposure to the atmosphere, the material was stored in the mother liquor (yield: 10−20% based on molybdenum). Anal. Calcd for $H_{48}N_7O_{56}NaMo_{16}$: Mo, 59.0; H, 1.85; N, 3.77. Found: Mo, 58.6; H, 1.98; N, 3.62. IR (KBr pellet, cm^{-1}): 1477 (s),

(26) Chae, H. K.; Klemperer, W. G.; Marquart, T. A. *Coord. Chem. Rev.* **1993**, *128*, 209.

Table 4. Selected Bond Lengths (Å) and Angles (deg) for **1**·4H_2O

Mo(1)−Na	3.556(3)	Mo(1)−O(1)	1.694(24)
Mo(1)−O(3)	1.890(36)	Mo(1)−O(4)	2.144(35)
Mo(1)−Mo(1C)	2.619(14)	Mo(1)−O(3A)	2.077(33)
Mo(1)−O(4A)	2.086(35)	Mo(1)−O(5C)	2.102(10)
Mo(2)−O(2A)	1.738(32)	Mo(2)−O(2B)	1.738(32)
Mo(2)−O(2C)	1.738(32)	Mo(2)−O(3B)	2.218(34)
Mo(2)−O(3C)	2.218(34)	Mo(2)−O(3D)	2.218(34)
Na−O(5A)	2.178(26)	Na−O(5B)	2.178(26)
Na−O(5C)	2.178(26)	Na−O(5D)	2.178(26)

O(1)−Mo(1)−O(3)	109.8(30)	O(1)−Mo(1)−O(4)	87.1(31)
O(3)−Mo(1)−O(4)	161.2(11)	O(1)−Mo(1)−O(3A)	101.9(30)
O(3)−Mo(1)−O(3A)	94.8(14)	O(4)−Mo(1)−O(3A)	89.5(11)
O(1)−Mo(1)−O(4A)	93.2(31)	O(3)−Mo(1)−O(4A)	85.0(11)
O(4)−Mo(1)−O(4A)	85.9(10)	O(3A)−Mo(1)−O(4A)	164.0(11)
O(1)−Mo(1)−O(5C)	156.1(30)	O(3)−Mo(1)−O(5C)	89.2(7)
O(4)−Mo(1)−O(5C)	72.5(10)	O(4A)−Mo(1)−O(5C)	73.6(11)
O(3A)−Mo(1)−O(5C)	90.4(7)	O(2A)−Mo(2)−O(2C)	103.6(9)
O(2A)−Mo(2)−O(2B)	103.6(9)	O(2A)−Mo(2)−O(3B)	161.5(9)
O(2B)−Mo(2)−O(2C)	103.6(9)	O(2C)−Mo(2)−O(3B)	87.8(12)
O(2B)−Mo(2)−O(3B)	87.3(12)	O(2B)−Mo(2)−O(3C)	161.5(9)
O(2A)−Mo(2)−O(3C)	87.8(12)	O(3B)−Mo(2)−O(3C)	78.1(7)
O(2C)−Mo(2)−O(3C)	87.3(12)	O(2B)−Mo(2)−O(3D)	87.8(12)
O(2A)−Mo(2)−O(3D)	87.3(12)	O(3B)−Mo(2)−O(3D)	78.1(7)
O(2C)−Mo(2)−O(3D)	161.5(9)	Mo(1)−O(3)−Mo(2A)	144.6(18)
O(3C)−Mo(2)−O(3D)	78.1(7)	Mo(1)−O(4)−Mo(1K)	105.4(15)
Mo(1)−O(3)−Mo(1C)	82.5(13)	Mo(1L)−O(5)−Mo(1M)	106.4(8)
Mo(1C)−O(3)−Mo(2A)	132.9(17)		

1110 (m), 1028 (m), 984 (m), 946 (vs), 842 (m), 786 (sh), 732 (vs), 557 (s), 535 (s), 488 (m).

Method B. Attempts to prepare **1** in the absence of organic cations and the pentaerythritol template resulted in improved yields of **1** but as microcrystalline materials unsuitable for X-ray determination. In a representative synthesis, a mixture of Na_2MoO_4·$2H_2O$, MoO_3, molybdenum metal (−325 mesh), NH_4Cl, and water in the mole ratio 6:6:4:20:300 was heated at 160 °C for 10 h to give **1**·4H_2O in 65% yield. Thermogravimetric analysis of **1** exhibited a 3% weight loss at 110−120 °C, consistent with the loss of 4 water molecules of crystallization (2.77% theoretical loss). UV/vis (solid state reflectance spectrum, nm): 325, 380. Magnetic susceptibility at room temperature: $\mu_{eff} = 1.2\ \mu_B$ (0.34 μ_B per Mo^V center). The infrared spectrum of this material was indistinguishable from that reported above for crystalline **1**·4H_2O.

$(Me_3NH)_4K_2[H_2Mo_{16}(OH)_{12}O_{40}]$·$8H_2O$ (2·$8H_2O$). A mixture of K_2MoO_4·$2H_2O$, MoO_3, Mo (−325 mesh), $(OHCH_2)_4C$, Me_3NHCl, Et_4NCl, and H_2O in the molar ratio 6:6:10:3:10:10:300 was placed in an autoclave which was subsequently heated for 4 days at 160 °C. The reaction mixture, which at this stage consists of an orange-red liquid and a brown powder, was allowed to stand at room temperature for 2 weeks, leading to the separation of orange-red plates in low yield (10−15%). These were filtered from the mother liquor and carefully separated from the brown powder. IR (KBr pellet, cm^{-1}): 1480(s), 1035(m), 979(m), 950(vs), 835(m), 738(vs), 570(s), 530(s).

$(Me_3NH)_2(Et_4N)Na_4[Na(H_2O)_3H_{15}Mo_{42}O_{109}\{(OCH_2)_3CCH_2OH\}_7]$·$15H_2O$ (3·$15H_2O$). Method A. Red-brown crystals of **3**·$15H_2O$ were filtered from the red-brown solution containing **1·4H_2O** described above, washed with water to remove orange-red amorphous solid, and dried at room temperature (yield: 55% based on Mo). IR (KBr pellet, cm^{-1}): 1171(w), 1112(vs), 1061(m), 1021(vs), 968(vs), 911(s), 886(s) 793(vs), 731(s, br), 646(m), 584(sh), 561(m), 536(m), 482(m). Anal. Calcd for $C_{49}H_{154}N_3O_{155}Na_5Mo_{42}$: C, 7.94; H, 2.08; Mo, 54.4. Found: C, 7.85; H, 2.23; Mo, 54.6.

Method B. A mixture of **1**·4H_2O, Na_2MoO_4·$2H_2O$, $C(CH_2OH)_4$, Me_3NHCl, Et_4NCl, and H_2O in the mole ratio 1:20:16:16:16:500 was placed in a 23 mL Parr acid digestion bomb and heated for 2 days at 160 °C. After the mixture was cooled to room temperature, dark red-brown plates of **3**·$15H_2O$ were collected in 70% yield.

$(Me_3NH)_2(H_3O)Na_6[Na(H_2O)_3H_{13}Mo_{42}O_{109}\{(OCH_2)_3CCH_2OH\}_7]$·$7H_2O$ (4·$7H_2O$). A mixture of Na_2MoO_4·$2H_2O$, MoO_3, $(HOCH_2)_4C$, Me_3NHCl, and H_2O in the mole ratio of 3:3:5:5:150 (pH adjusted to *ca.* 6 by addition of HCl) was placed in an autoclave which was subsequently heated for 3 days at 160 °C. After the vessel was cooled to room temperature, red-brown crystals of **4**·$7H_2O$ were filtered from the orange-red mother liquor, washed with water, and air-dried

Table 5. Selected Bond Lengths (Å) and Angles (deg) for **2**·$8H_2O$

Mo(1)−O(1)	1.970(8)	Mo(1)−O(6)	2.119(11)
Mo(1)−O(10)	1.684(13)	Mo(1)−O(12)	2.105(8)
Mo(1)−Mo(1A)	2.594(3)	Mo(1)−O(1A)	1.970(8)
Mo(1)−O(12A)	2.105(8)	Mo(2)−O(3)	2.119(12)
Mo(2)−O(4)	1.980(8)	Mo(2)−O(9)	2.116(8)
Mo(2)−O(11)	1.666(12)	Mo(2)−Mo(2B)	2.602(3)
Mo(2)−K(1A)	3.957(8)	Mo(2)−O(4A)	1.980(8)
Mo(2)−O(9C)	2.116(8)	Mo(3)−Mo(4)	2.592(2)
Mo(3)−O(2)	1.961(8)	Mo(3)−O(3)	2.112(7)
Mo(3)−O(5)	1.970(7)	Mo(3)−O(8)	2.110(7)
Mo(3)−O(15)	1.696(8)	Mo(3)−K(1A)	3.956(7)
Mo(3)−O(9C)	2.133(8)	Mo(4)−O(2)	1.971(7)
Mo(4)−O(5)	1.956(8)	Mo(4)−O(6)	2.137(7)
Mo(4)−O(7)	2.115(6)	Mo(4)−O(12)	2.111(8)
Mo(4)−O(18)	1.687(8)	Mo(5)−O(5)	2.232(7)
Mo(5)−O(4A)	2.160(11)	Mo(5)−O(5A)	2.232(7)
Mo(5)−O(13A)	1.771(11)	Mo(5)−O(16A)	1.738(9)
Mo(5)−O(16B)	1.738(9)	Mo(6)−O(1)	2.233(11)
Mo(6)−O(2)	2.224(8)	Mo(6)−O(14)	1.740(12)
Mo(6)−O(17)	1.746(8)	Mo(6)−K(1B)	3.597(8)
Mo(6)−O(2A)	2.224(8)	Mo(6)−O(17A)	1.746(8)
K(1)−O(8A)	2.920(14)	K(1)−O(9A)	2.911(10)
K(1)−O(9B)	2.911(10)	K(1)−O(17B)	2.866(11)
K(1)−O(17C)	2.866(11)	K(1)−O(20A)	2.869(38)
K(1)−O(20B)	2.869(38)	K(1)−O(21A)	2.837(50)

O(1)−Mo(1)−O(6)	88.3(4)	O(1)−Mo(1)−O(10)	105.2(4)
O(6)−Mo(1)−O(10)	159.8(5)	O(1)−Mo(1)−O(12)	85.8(3)
O(6)−Mo(1)−O(12)	74.2(3)	O(10)−Mo(1)−O(12)	91.5(4)
O(1)−Mo(1)−O(1A)	94.8(5)	O(6)−Mo(1)−O(1A)	88.3(4)
O(10)−Mo(1)−O(1A)	105.2(4)	O(12)−Mo(1)−O(1A)	162.5(4)
O(6)−Mo(1)−O(12A)	74.2(3)	O(1)−Mo(1)−O(12A)	162.5(4)
O(12)−Mo(1)−O(12A)	88.4(4)	O(10)−Mo(1)−O(12A)	91.5(4)
O(1A)−Mo(1)−O(12A)	85.8(3)	O(3)−Mo(2)−O(4)	88.4(4)
O(3)−Mo(2)−O(9)	74.5(3)	O(4)−Mo(2)−O(9)	86.6(3)
O(3)−Mo(20−O(11)	159.2(5)	O(4)−Mo(2)−O(11)	105.4(4)
O(9)−Mo(2)−O(11)	90.7(4)	O(3)−Mo(2)−O(4A)	88.4(4)
O(4)−Mo(2)−O(4A)	94.7(4)	O(9)−Mo(2)−O(4A)	162.8(4)
O(11)−Mo(2)−O(4A)	105.4(4)	O(3)−Mo(2)−O(9C)	74.5(3)
O(4)−Mo(2)−O(9C)	162.8(4)	O(9)−Mo(2)−O(9C)	87.3(4)
O(11)−Mo(2)−O(9C)	90.7(4)	O(3)−Mo(3)−O(5)	89.1(3)
O(3)−Mo(3)−O(15)	158.2(4)	O(2)−Mo(3)−O(8)	86.4(4)
O(8)−Mo(3)−O(15)	91.0(4)	O(5)−Mo(3)−O(8)	163.1(5)
O(2)−Mo(3)−O(9C)	163.7(3)	O(2)−Mo(3)−O(15)	105.6(4)
O(5)−Mo(3)−O(9C)	87.0(3)	O(5)−Mo(3)−O(15)	104.8(3)
O(15)−Mo(3)−O(9C)	89.5(4)	O(3)−Mo(3)−O(9C)	74.3(4)
O(2)−Mo(3)−O(3)	89.6(4)	O(8)−Mo(3)−O(9C)	87.3(4)
O(2)−Mo(3)−O(5)	94.8(3)	O(5)−Mo(4)−O(6)	88.8(4)
O(2)−Mo(4)−O(5)	94.9(3)	O(2)−Mo(4)−O(7)	163.3(3)
O(2)−Mo(4)−O(6)	89.0(3)	O(6)−Mo(4)−O(7)	74.3(3)
O(5)−Mo(4)−O(12)	162.5(3)	O(2)−Mo(4)−O(12)	86.2(3)
O(7)−Mo(4)−O(12)	88.1(4)	O(6)−Mo(4)−O(12)	73.8(4)
O(2)−Mo(4)−O(18)	105.3(4)	O(5)−Mo(4)−O(18)	105.4(4)
O(6)−Mo(4)−O(18)	158.6(4)	O(7)−Mo(4)−O(18)	90.4(4)
O(12)−Mo(4)−O(18)	91.1(4)	O(5)−Mo(5)−O(4A)	78.1(3)
O(5)−Mo(5)−O(5A)	77.0(4)	O(4A)−Mo(5)−O(5A)	78.1(3)
O(5)−Mo(5)−O(13A)	85.1(3)	O(4A)−Mo(5)−O(13A)	158.5(5)
O(5A)−Mo(5)−O(13A)	85.1(3)	O(5)−Mo(5)−O(16A)	87.4(3)
O(4A)−Mo(5)−O(16A)	89.2(3)	O(5A)−Mo(5)−O(16A)	161.6(3)
O(13A)−Mo(5)−O(16A)	103.6(3)	O(5)−Mo(5)−O(16B)	161.6(3)
O(4A)−Mo(5)−O(16B)	89.2(3)	O(5A)−Mo(5)−O(16B)	87.4(3)
O(13A)−Mo(5)−O(16B)	103.6(3)	O(16A)−Mo(5)−O(16B)	106.0(6)
O(1)−Mo(6)−O(2)	77.7(3)	O(1)−Mo(6)−O(14)	160.6(5)
O(2)−Mo(6)−O(14)	87.3(4)	O(1)−Mo(6)−O(17)	86.8(3)
O(2)−Mo(6)−O(17)	160.5(3)	O(14)−Mo(6)−O(17)	104.9(4)
O(1)−Mo(6)−O(2A)	77.7(3)	O(2)−Mo(6)−O(2A)	77.8(4)
O(14)−Mo(6)−O(2A)	87.3(4)	O(17)−Mo(6)−O(2A)	87.5(3)
O(1)−Mo(6)−O(17A)	86.8(3)	O(2)−Mo(6)−O(17A)	87.5(3)
O(14)−Mo(6)−O(17A)	104.9(4)	O(17)−Mo(6)−O(17A)	103.5(6)
O(2A)−Mo(6)−O(17A)	160.5(3)		

(yield: 60−65% based on molybdenum). The orange-red mother liquor, on standing, produced cubic crystals of $(NH_4)_7[NaMo_{16}(OH)_{12}O_{40}]$ in low yield. IR (KBr pellet, cm^{-1}): 1110(vs), 1015(vs), 975(vs), 918(s), 890(s), 785(vs), 650(m), 560(m). Anal. Calcd for $C_{41}H_{119}N_2O_{148}Na_7Mo_{42}$: Mo, 56.0. Found: Mo, 55.8.

$Na_9[(MoO_3)H_{14}Mo_{42}O_{109}\{(OCH_2)_3CCH_2OH\}_7]$·$0.5C(CH_2OH)_4$·$25H_2O$ (5·$0.5C(CH_2OH)_4$·$25H_2O$). An autoclave was loaded with a mixture of Na_2MoO_4·$2H_2O$, MoO_3, $(HOCH_2)_4C$, NaCl, and H_2O

Table 6. Atomic Positional Parameters ($\times 10^4$) and Isotropic Temperature Factors (Å^2 $\times$ 10^3) for the Molecular Anion and the Sodium Cations of $(Me_3NH)_2(Et_4N)Na_4$ $[Na(H_2O)_3H_{15}Mo_{42}O_{109}\{(OCH_2)_3CCH_2OH\}_7]\cdot 15H_2O$ (**3**·$15H_2O$)

	x	*y*	*z*	*U*(eq)[a]		*x*	*y*	*z*	*U*(eq)[a]
Mo(1)	3948(1)	9454(1)	2761(1)	28(1)	O(28)	5344(6)	7902(4)	1540(7)	25(3)
Mo(2)	4689(1)	9023(1)	4062(1)	26(1)	O(29)	5932(6)	8476(4)	3041(7)	32(3)
Mo(3)	3303(1)	8817(1)	947(1)	30(1)	O(30)	6461(6)	8424(5)	1785(8)	36(3)
Mo(4)	1788(1)	8841(1)	2561(1)	32(1)	O(31)	6258(6)	7397(4)	2933(7)	27(3)
Mo(5)	2350(1)	9372(1)	1929(1)	32(1)	O(32)	6578(6)	7389(4)	1678(7)	29(3)
Mo(6)	3507(1)	7840(1)	775(1)	29(1)	O(33)	7162(6)	7987(4)	3207(7)	29(3)
Mo(7)	5088(1)	8484(1)	2135(1)	27(1)	O(34)	8030(7)	7481(5)	4537(8)	41(3)
Mo(8)	6211(1)	8047(1)	2268(1)	28(1)	O(35)	2591(6)	8253(5)	5084(8)	34(3)
Mo(9)	7221(1)	7465(1)	4025(1)	29(1)	O(36)	6805(6)	7987(4)	4567(7)	26(3)
Mo(10)	6811(1)	7454(1)	5193(1)	29(1)	O(37)	6933(6)	6933(5)	4388(8)	33(3)
Mo(11)	6507(1)	6724(1)	2119(1)	28(1)	O(38)	7533(6)	7469(5)	5967(8)	36(3)
Mo(12)	5570(1)	6180(1)	1872(1)	28(1)	O(39)	6417(6)	6916(5)	5529(8)	34(3)
Mo(13)	3063(1)	9666(1)	4237(1)	29(1)	O(40)	5695(6)	7454(5)	4225(8)	34(3)
Mo(14)	2968(1)	9952(1)	5637(1)	31(1)	O(41)	6281(6)	7948(4)	5775(8)	33(3)
Mo(15)	1789(1)	8355(1)	5694(1)	35(1)	O(42)	6927(6)	6364(5)	1621(8)	36(3)
Mo(16)	2250(1)	9180(1)	6465(1)	35(1)	O(43)	5620(6)	6760(4)	1372(7)	31(3)
Mo(17)	4773(1)	8597(1)	7250(1)	33(1)	O(44)	6355(6)	6324(5)	2835(8)	34(3)
Mo(18)	3947(1)	9327(1)	7367(1)	34(1)	O(45)	5789(6)	5688(4)	1323(8)	34(3)
Mo(19)	1681(1)	8274(1)	371(1)	34(1)	O(46)	4564(6)	6214(4)	1125(7)	30(3)
Mo(20)	771(1)	7725(1)	−584(1)	41(1)	O(47)	5091(6)	6832(4)	2553(7)	28(3)
Mo(21)	406(1)	7012(1)	1818(1)	40(1)	O(48)	5291(6)	5834(5)	2628(8)	36(3)
Mo(22)	30(1)	6990(1)	252(1)	46(1)	O(49)	2965(6)	10233(5)	3920(8)	36(3)
Mo(23)	2175(1)	5979(1)	47(1)	38(1)	O(50)	3231(6)	8830(4)	4433(7)	29(3)
Mo(24)	1063(1)	6406(1)	−770(1)	45(1)	O(51)	3710(6)	9738(4)	5345(8)	32(3)
Mo(25)	2806(1)	7159(1)	1614(1)	30(1)	O(52)	2341(6)	9675(5)	4622(8)	38(3)
Mo(26)	2067(1)	7594(1)	2373(1)	30(1)	O(53)	2864(6)	10587(5)	5620(8)	34(3)
Mo(27)	2727(1)	8246(1)	4193(1)	29(1)	O(54)	3122(6)	9200(4)	6116(7)	31(3)
Mo(28)	3978(1)	8338(1)	4838(1)	27(1)	O(55)	3611(6)	10024(4)	6894(8)	34(3)
Mo(29)	4940(1)	7788(1)	3866(1)	24(1)	O(56)	2248(6)	9916(5)	6152(8)	35(3)
Mo(30)	4427(1)	7268(1)	2457(1)	25(1)	O(57)	1175(7)	8365(5)	6025(8)	42(3)
Mo(31)	1126(1)	8176(1)	3312(1)	33(1)	O(58)	1715(6)	9007(5)	5341(8)	35(3)
Mo(32)	643(1)	7580(1)	3956(1)	35(1)	O(59)	2184(7)	5490(5)	−627(8)	40(3)
Mo(33)	1861(1)	6994(1)	5552(1)	43(1)	O(60)	1266(6)	8105(4)	4470(8)	35(3)
Mo(34)	1159(1)	6320(1)	3622(1)	47(1)	O(61)	2551(7)	8489(5)	6679(8)	40(3)
Mo(35)	5575(1)	8503(1)	5626(1)	26(1)	O(62)	2147(7)	7622(5)	5790(8)	41(3)
Mo(36)	6253(1)	8000(1)	6894(1)	31(1)	O(63)	1714(7)	9367(5)	6935(9)	47(4)
Mo(37)	5310(1)	7270(1)	7387(1)	41(1)	O(64)	3052(6)	9403(5)	7561(8)	37(3)
Mo(38)	6341(1)	6713(1)	6414(1)	43(1)	O(65)	5335(7)	8712(5)	8186(9)	50(4)
Mo(39)	3764(1)	6653(1)	647(1)	28(1)	O(66)	5419(6)	8423(5)	6623(8)	38(3)
Mo(40)	3960(1)	5666(1)	636(1)	29(1)	O(33)	7162(6)	7987(4)	3207(7)	29(3)
Mo(41)	3132(1)	5206(1)	1691(1)	40(1)	O(34)	8030(7)	7481(5)	4537(8)	41(3)
Mo(42)	4833(1)	5313(1)	2609(1)	42(1)	O(35)	2591(6)	8253(5)	5084(8)	34(3)
Na(1)	3658(3)	6938(2)	3987(4)	26(3)	O(36)	6805(6)	7987(4)	4567(7)	26(3)
Na(2)	5185(4)	329(3)	4049(5)	35(3)	O(37)	6933(6)	6933(5)	4388(8)	33(3)
Na(3)	4937(4)	7276(3)	424(5)	48(4)	O(38)	7533(6)	7469(5)	5967(8)	36(3)
Na(4)	6364(4)	8809(3)	4385(5)	42(4)	O(39)	6417(6)	6916(5)	5529(8)	34(3)
Na(5)	1286(4)	9394(3)	4135(6)	61(4)	O(40)	5695(6)	7454(5)	4225(8)	34(3)
O(1)	4356(6)	9974(5)	2977(8)	34(3)	O(41)	6281(6)	7948(4)	5775(8)	33(3)
O(2)	3833(6)	9402(4)	3802(7)	31(3)	O(42)	6927(6)	6364(5)	1621(8)	36(3)
O(3)	4664(6)	8930(4)	2915(7)	27(3)	O(43)	5620(6)	6760(4)	1372(7)	31(3)
O(4)	3249(6)	8949(4)	2108(7)	32(3)	O(44)	6355(6)	6324(5)	2835(8)	34(3)
O(5)	3063(6)	9884(4)	2394(8)	33(3)	O(45)	5789(6)	5688(4)	1323(8)	34(3)
O(6)	3877(6)	9412(4)	1539(7)	30(3)	O(46)	4564(6)	6214(4)	1125(7)	30(3)
O(7)	5201(6)	9483(4)	4476(8)	33(3)	O(47)	5091(6)	6832(4)	2553(7)	28(3)
O(8)	4668(6)	8886(4)	5151(7)	29(3)	O(48)	5291(6)	5834(5)	2628(8)	36(3)
O(9)	4171(6)	8353(4)	3753(7)	30(3)	O(49)	2965(6)	10233(5)	3920(8)	36(3)
O(10)	5419(6)	8462(4)	4401(7)	27(3)	O(50)	3231(6)	8830(4)	4433(7)	29(3)
O(11)	3282(7)	8935(5)	42(8)	39(3)	O(51)	3710(6)	9738(4)	5345(8)	32(3)
O(12)	4089(6)	8383(4)	1368(8)	34(3)	O(52)	2341(6)	9675(5)	4622(8)	38(3)
O(13)	2704(6)	8282(5)	649(8)	34(3)	O(53)	2864(6)	10587(5)	5620(8)	34(3)
O(14)	2500(6)	9348(5)	815(8)	36(3)	O(54)	3122(6)	9200(4)	6116(7)	31(3)
O(15)	1106(7)	9220(5)	2425(8)	44(4)	O(55)	3611(6)	10024(4)	6894(8)	34(3)
O(16)	2577(6)	8253(4)	2928(7)	30(3)	O(56)	2248(6)	9916(5)	6152(8)	35(3)
O(17)	1848(6)	8675(5)	3704(8)	37(3)	O(57)	1175(7)	8365(5)	6025(8)	42(3)
O(18)	1873(6)	8759(5)	1465(8)	36(3)	O(58)	1715(6)	9007(5)	5341(8)	35(3)
O(19)	2465(6)	9323(4)	3078(8)	33(3)	O(59)	2184(7)	5490(5)	−627(8)	40(3)
O(20)	1326(6)	8186(4)	2259(8)	33(3)	O(60)	1266(6)	8105(4)	4470(8)	35(3)
O(21)	1765(6)	9826(5)	1623(8)	36(3)	O(61)	2551(7)	8489(5)	6679(8)	40(3)
O(22)	3531(7)	7783(5)	−171(8)	39(3)	O(62)	2147(7)	7622(5)	5790(8)	41(3)
O(23)	4255(6)	7290(4)	1207(7)	29(3)	O(63)	1714(7)	9367(5)	6935(9)	47(4)
O(24)	3508(6)	7726(4)	1984(7)	30(3)	O(64)	3052(6)	9403(5)	7561(8)	37(3)
O(25)	3003(6)	7210(4)	560(7)	30(3)	O(65)	5335(7)	8712(5)	8186(9)	50(4)
O(26)	5113(6)	8957(5)	1648(8)	37(3)	O(66)	5419(6)	8423(5)	6623(8)	38(3)
O(27)	4842(6)	7907(4)	2756(7)	32(3)	O(67)	4757(6)	7823(5)	7171(8)	37(3)

Table 6 (Continued)

	x	*y*	*z*	*U*(eq)[a]		*x*	*y*	*z*	*U*(eq)[a]
O(68)	3948(6)	8620(5)	7419(8)	35(3)	O(117)	6187(7)	6804(5)	7535(9)	47(4)
O(69)	4544(6)	9239(4)	6808(7)	31(3)	O(118)	5735(8)	6307(6)	5973(9)	54(4)
O(70)	4075(6)	8363(4)	5859(7)	31(3)	O(119)	7049(8)	6350(6)	6843(10)	61(4)
O(71)	4345(7)	9575(5)	8348(9)	49(4)	O(120)	3782(6)	6700(5)	−270(8)	38(3)
O(72)	1497(7)	8748(5)	−202(9)	46(4)	O(121)	4012(7)	5501(5)	−279(8)	39(3)
O(73)	2130(6)	7724(5)	1346(8)	36(3)	O(122)	3909(7)	5729(5)	1901(8)	39(3)
O(74)	1700(6)	7697(5)	−407(8)	39(3)	O(123)	4702(7)	5189(5)	1290(8)	39(3)
O(75)	856(6)	8141(5)	433(8)	37(3)	O(124)	3385(6)	5117(4)	572(7)	31(3)
O(76)	374(7)	8079(5)	−1350(9)	52(4)	O(125)	2758(7)	4652(5)	1393(9)	51(4)
O(77)	1008(6)	7060(4)	161(7)	32(3)	O(126)	3164(8)	5374(6)	2682(10)	64(5)
O(78)	705(7)	7056(5)	−1412(9)	46(4)	O(127)	4690(8)	5453(6)	3489(9)	57(4)
O(79)	−138(7)	7518(5)	−606(8)	44(4)	O(128)	5391(8)	4815(6)	2823(10)	65(5)
O(80)	−320(7)	6943(5)	1865(9)	50(4)	O(129)	4072(7)	4816(5)	2122(9)	45(4)
O(81)	672(6)	7557(5)	2836(8)	36(3)	O(130)	7406(6)	6928(4)	3099(7)	28(3)
O(82)	1490(6)	7169(5)	2031(8)	34(3)	C(1)	3049(11)	10141(8)	1067(13)	47(6)
O(83)	211(7)	7546(5)	1099(8)	41(4)	C(2)	2498(10)	9817(7)	518(12)	40(5)
O(84)	998(7)	6522(5)	2634(9)	45(4)	C(3)	2983(11)	10301(8)	1921(13)	48(6)
O(85)	497(7)	6499(5)	962(8)	42(3)	C(4)	3733(10)	9877(7)	1180(13)	43(5)
O(86)	−785(7)	6923(5)	−66(9)	51(4)	C(5)	2991(11)	10643(8)	683(14)	55(6)
O(87)	106(7)	6465(5)	−750(9)	49(4)	C(6)	7793(10)	7487(7)	2411(12)	34(5)
O(88)	1750(8)	6878(5)	6398(9)	55(4)	C(7)	7200(10)	7437(8)	1586(13)	50(6)
O(89)	1943(7)	6556(5)	−577(8)	42(4)	C(8)	7712(10)	7961(7)	2930(12)	36(5)
O(90)	2493(7)	5664(5)	1113(8)	39(3)	C(9)	7911(10)	7022(7)	2844(12)	36(5)
O(91)	3156(6)	6127(5)	386(8)	35(3)	C(10)	8370(11)	7562(8)	2164(14)	52(6)
O(92)	1339(6)	6006(5)	143(8)	39(3)	C(11)	2805(9)	10323(7)	7585(12)	33(5)
O(93)	2343(6)	6657(5)	1133(8)	37(3)	C(12)	3434(9)	10422(7)	7414(11)	30(4)
O(94)	812(7)	6025(5)	−1659(9)	49(4)	C(13)	2232(10)	10319(7)	6814(11)	35(5)
O(95)	2871(6)	7186(4)	2729(7)	28(3)	C(14)	2932(10)	9854(7)	8029(12)	35(5)
O(96)	3709(6)	6766(4)	1891(7)	30(3)	C(15)	2687(11)	10779(8)	8184(13)	49(6)
O(97)	2069(6)	7704(5)	3568(8)	36(3)	C(16)	−482(11)	6944(8)	−1900(14)	48(6)
O(98)	3464(6)	7768(4)	4316(7)	30(3)	C(17)	−641(11)	7421(8)	−1436(14)	56(6)
O(99)	4866(6)	7886(4)	5026(7)	30(3)	C(18)	−425(12)	6517(9)	−1558(14)	62(7)
O(100)	4311(6)	7284(4)	3482(7)	30(3)	C(19)	99(11)	7016(9)	−2131(14)	54(6)
O(101)	506(7)	8611(5)	3086(9)	49(4)	C(20)	−1087(14)	6939(10)	−2758(17)	75(8)
O(102)	−83(6)	7882(5)	3841(8)	39(3)	C(21)	152(11)	6715(8)	4864(14)	47(6)
O(103)	1563(7)	7065(5)	4221(8)	42(4)	C(22)	350(10)	7221(8)	5320(13)	43(5)
O(104)	323(7)	6872(5)	3621(8)	42(4)	C(23)	−125(10)	6723(8)	3933(13)	47(6)
O(105)	876(7)	7402(5)	5120(9)	45(4)	C(24)	694(11)	6298(9)	5049(14)	57(6)
O(106)	2552(7)	6637(5)	5575(9)	52(4)	C(25)	−401(13)	6568(10)	5100(16)	70(8)
O(107)	1904(8)	6021(6)	3841(10)	63(5)	C(26)	7095(10)	7286(8)	8556(13)	41(5)
O(108)	657(8)	5848(5)	3419(9)	55(4)	C(27)	7369(11)	7339(8)	7871(13)	49(6)
O(109)	1240(7)	6406(5)	4854(9)	49(4)	C(28)	6715(11)	6832(8)	8314(14)	54(6)
O(110)	6002(6)	9013(5)	5925(8)	34(3)	C(29)	6639(11)	7731(8)	8633(13)	49(6)
O(111)	6810(6)	8396(5)	7455(8)	36(3)	C(30)	7635(15)	7259(12)	9381(19)	94(10)
O(112)	5639(7)	7350(5)	6400(8)	39(3)	C(31)	4182(10)	4376(7)	820(12)	34(5)
O(113)	6075(7)	7800(5)	7875(8)	41(3)	C(32)	3555(9)	4627(7)	287(12)	35(5)
O(114)	6895(6)	7370(5)	7087(8)	38(3)	C(33)	4161(11)	4330(8)	1682(12)	44(5)
O(115)	537(7)	7192(5)	8381(9)	55(4)	C(34)	4760(10)	4673(7)	912(12)	36(5)
O(116)	4820(8)	6808(6)	6792(9)	56(4)	C(35)	4296(11)	3868(8)	432(14)	48(6)

[a] Equivalent isotropic *U* defined as one-third of the trace of the orthogonalized $\mathbf{U}_{ij}$ tensor.

in the mole ratio 3:3:5:10:170. After the vessel was heated for 3 days at 160 °C, the contents were cooled to room temperature over a period of 6−10 h. The orange-red barlike crystals were filtered from the orange-red mother liquor and stored in few drops of the mother liquor (yield: 60% based on molybdenum). IR (KBr pellet, cm^{-1}): 1192-(w), 1110(vs), 1056(m), 1018(s), 964(s), 915(s), 877(w), 861(w), 794-(s, br), 740(br), 650(m), 582(w). Anal. Calcd for $C_{37.5}H_{133}O_{167}Na_9Mo_{43}$: Mo, 54.4. Found: Mo, 54.6. Thermogravimetric analysis of **5** revealed a weight loss of 6.5% between 90 and 120 °C, corresponding to the removal of the H_2O molecules of crystallization (5.9% theoretical for 25 H_2O molecules).

$(Me_4N)(Et_2NH_2)(H_3O)_2Na_6[(MoO_3)H_{13}Mo_{42}O_{109}\{(OCH_2)_3CCH_3\}_7]\cdot 10H_2O$ (6·10H_2O). Method A. An autoclave was charged with a mixture of $Na_2MoO_4\cdot 2H_2O$, MoO_3, $(HOCH_2)_3CCH_3$, Me_4NCl, Et_2NH, and H_2O in the mole ratio 6:6:10:10:10:300 (pH adjusted to *ca*. 6 by addition of HCl). After the reaction vessel was heated for 3 days at 160 °C, the contents were cooled to room temperature. Bright red-brown, flat, rodlike crystals were filtered from the red mother liquor, thoroughly washed with water to remove minor amounts of yellow amorphous solid, and air-dried to give 70−75% yield of air-stable and water-insoluble crystalline material. No other products could be isolated from the dark-red mother liquor. IR (KBr pellet, cm^{-1}): 1171(w), 1124(s), 1035(vs), 968(s), 920(vs), 887(s), 789(vs), 739(m), 557(w), 538(w), 488(w). Anal. Calcd for $C_{43}H_{126}N_2Na_6O_{145}Mo_{43}$: Mo, 56.9. Found: Mo, 57.2.

Method B. A mixture of **1**·4H_2O, $Na_2MoO_4\cdot 2H_2O$, MoO_3, Me_4NCl, Et_2NH, $(HOCH_2)_3CCH_3$, and H_2O in the mole ratio 1:20:20:16:16:16:300 was heated for 5 h at 160 °C. After the mixture was cooled to room temperature, dark red-brown plates of **6**·10H_2O were isolated in 65% yield.

X-ray Crystallographic Studies. The experimental X-ray data for **1**−**6** are summarized in Table 1. Full lists of atomic positional parameters for **1**·4H_2O and **2**·8H_2O are presented in Tables 2 and 3, respectively, while Tables 4 and 5 list selected bond lengths and angles. Atomic coordinates for the anionic clusters and sodium cations of **3**·15H_2O, **4**·7H_2O, **5**·25H_2O·0.5$C(CH_2OH)_4$, and **6**·10H_2O are listed in Tables 6−9, respectively.

Data for the structural studies of **1**·4H_2O, **2**·8H_2O, **3**·15H_2O, and **5**·25H_2O·0.5$C(CH_2OH)_4$ were collected on a Rigaku AFC5S diffractometer, using the $\omega/2\theta$ scan mode for **1**·4H_2O and **2**·8H_2O and the ω scan mode for **3**·15H_2O and **5**·25H_2O·0.5$C(CH_2OH)_4$.

The small size of the crystals and weak diffraction profiles associated with compound **4**·7H_2O required data collection on a high-flux instrument. Consequently, data were collected on the Rigaku AFC7R

Table 7. Atomic Positional Parameters ($\times 10^4$) and Isotropic Temperature Factors (Å^2 $\times$ 10^3) for the Molecular Anion and the Sodium Cations of $(Me_3NH)_2(H_3O)Na_6[Na(H_2O)_3H_{13}Mo_{42}O_{109}\{(OCH_2)_3CH_2OH\}_7]\cdot 7H_2O$ (**4**·$7H_2O$)

	x	*y*	*z*	*U*(eq)[a]		*x*	*y*	*z*	*U*(eq)[a]
Mo(1)	744(1)	4756(1)	6292(1)	21(1)	O(26)	2404(3)	2716(11)	3532(5)	27(5)
Mo(2)	796(1)	6132(1)	6084(1)	22(1)	O(27)	1978(3)	3069(10)	3915(5)	23(4)
Mo(3)	1205(1)	3415(1)	6134(1)	22(1)	O(28)	1866(3)	4105(10)	3304(5)	24(4)
Mo(4)	1590(1)	3782(1)	5826(1)	22(1)	O(29)	2305(3)	4263(10)	3780(5)	25(5)
Mo(5)	632(1)	3313(1)	5635(1)	20(1)	O(30)	1934(4)	2692(11)	3178(5)	30(5)
Mo(6)	604(1)	3626(1)	4947(1)	18(1)	O(31)	2288(4)	3845(11)	3040(5)	31(5)
Mo(7)	2177(1)	3358(1)	3531(1)	26(1)	O(32)	2193(3)	4863(10)	2469(5)	23(4)
Mo(8)	2198(1)	3745(1)	4206(1)	24(1)	O(33)	2183(3)	5357(11)	3222(5)	26(5)
Mo(9)	2035(1)	4724(1)	2844(1)	26(1)	O(34)	1751(3)	5331(11)	2764(5)	27(5)
Mo(10)	1952(1)	6098(1)	3023(1)	27(1)	O(35)	1826(3)	3805(11)	2621(5)	27(5)
Mo(11)	1611(1)	3295(1)	3020(1)	24(1)	O(36)	1512(4)	2606(11)	2717(5)	31(5)
Mo(12)	1215(1)	3619(1)	3313(1)	21(1)	O(37)	1488(3)	3014(10)	3486(4)	19(4)
Mo(13)	311(1)	9200(1)	4108(1)	23(1)	O(38)	1387(3)	4130(10)	2942(5)	21(4)
Mo(14)	535(1)	8868(1)	4725(1)	23(1)	O(39)	2431(4)	3193(11)	4355(5)	31(5)
Mo(15)	194(1)	7781(1)	3443(1)	21(1)	O(40)	1986(3)	3539(10)	4647(5)	24(4)
Mo(16)	325(1)	6407(1)	3584(1)	19(1)	O(41)	1847(3)	4529(10)	4096(5)	22(4)
Mo(17)	627(1)	9211(1)	3300(1)	25(1)	O(42)	2278(3)	4730(10)	4475(5)	24(5)
Mo(18)	1081(1)	8895(1)	3314(1)	25(1)	O(43)	2100(3)	6510(10)	2693(5)	24(5)
Mo(19)	724(1)	3214(1)	3960(1)	19(1)	O(44)	1717(3)	5698(10)	3509(5)	24(4)
Mo(20)	1145(1)	3232(1)	4341(1)	19(1)	O(45)	1643(3)	6827(10)	2991(4)	19(4)
Mo(21)	317(1)	4544(1)	4093(1)	17(1)	O(46)	2077(3)	6794(11)	3452(5)	29(5)
Mo(22)	391(1)	5616(1)	4580(1)	16(1)	O(47)	1032(3)	3012(10)	3805(4)	15(4)
Mo(23)	596(1)	4524(1)	3327(1)	21(1)	O(48)	1052(3)	3376(9)	3805(4)	15(4)
Mo(24)	907(1)	5600(1)	3188(1)	21(1)	O(49)	950(3)	4496(10)	3258(4)	20(4)
Mo(25)	1019(1)	6939(1)	3818(1)	19(1)	O(50)	1383(3)	4531(10)	3683(4)	19(4)
Mo(26)	793(1)	6925(1)	4417(1)	17(1)	O(51)	128(3)	9894(11)	4245(5)	29(5)
Mo(27)	1545(1)	4630(1)	4178(1)	19(1)	O(52)	268(3)	8367(10)	4437(5)	22(4)
Mo(28)	1438(1)	5638(1)	3682(1)	20(1)	O(53)	641(3)	9440(10)	4315(5)	25(5)
Mo(29)	1252(1)	4637(1)	4957(1)	17(1)	O(54)	498(3)	8400(10)	3730(5)	23(4)
Mo(30)	922(1)	5643(1)	5057(1)	16(1)	O(55)	397(3)	9827(10)	3642(5)	25(5)
Mo(31)	613(1)	7969(1)	5651(1)	23(1)	O(56)	45(3)	8682(10)	3743(5)	24(4)
Mo(32)	482(1)	6893(1)	5170(1)	18(1)	O(57)	−67(3)	7640(10)	3176(5)	23(4)
Mo(33)	1072(1)	9107(1)	5361(1)	35(1)	O(58)	174(3)	7147(10)	3872(4)	19(4)
Mo(34)	1202(1)	7758(2)	6028(1)	36(1)	O(59)	426(4)	7152(11)	3229(5)	31(5)
Mo(35)	2074(1)	3504(1)	5183(1)	22(1)	O(60)	295(3)	8682(10)	3095(5)	22(4)
Mo(36)	1652(1)	3332(1)	4799(1)	20(1)	O(61)	606(3)	9919(11)	2979(5)	28(5)
Mo(37)	2087(1)	5132(1)	5735(1)	28(1)	O(62)	894(3)	9454(11)	3651(5)	27(5)
Mo(38)	2394(1)	5103(2)	4923(1)	32(1)	O(63)	794(3)	8381(10)	3082(5)	22(4)
Mo(39)	1620(1)	7952(1)	2970(1)	26(1)	O(64)	396(3)	9509(11)	4983(5)	27(5)
Mo(40)	1289(1)	6882(1)	3036(1)	23(1)	O(65)	523(3)	7989(10)	5108(5)	24(5)
Mo(41)	1698(1)	9120(1)	3737(1)	31(1)	O(66)	887(3)	8996(10)	4932(5)	25(5)
Mo(42)	2131(1)	7760(2)	3578(1)	34(1)	O(67)	752(3)	7881(10)	4458(5)	24(4)
Na(1)	4961(2)	2253(6)	549(3)	25(4)	O(68)	95(3)	5958(10)	3356(5)	26(5)
Na(2)	697(2)	7292(7)	2773(3)	35(4)	O(69)	585(3)	5636(10)	3385(5)	24(4)
Na(3)	1640(2)	2273(6)	3984(3)	32(4)	O(70)	668(3)	6750(9)	3905(4)	14(4)
Na(4)	1187(2)	2314(7)	5191(3)	35(4)	O(71)	334(4)	5637(10)	4032(5)	22(4)
Na(5)	257(2)	4817(6)	470(3)	21(3)	O(72)	1159(4)	9532(12)	3000(5)	35(5)
Na(6)	1402(3)	4368(10)	957(4)	54(6)	O(73)	1371(3)	7978(10)	3125(5)	22(4)
Na(7)	1495(1)	6615(4)	4654(2)	48(3)	O(74)	1287(3)	7978(10)	3125(5)	22(4)
O(1)	612(3)	4892(11)	6692(5)	26(5)	O(75)	1025(3)	7872(10)	3742(4)	19(4)
O(2)	921(3)	4141(9)	5827(4)	16(4)	O(76)	687(3)	2289(10)	3921(5)	25(5)
O(3)	565(3)	5345(10)	5925(5)	24(5)	O(77)	671(3)	4375(10)	3888(5)	22(4)
O(4)	1031(3)	5412(10)	6304(4)	19(4)	O(78)	358(3)	3349(10)	4073(4)	16(4)
O(5)	987(3)	3905(10)	6522(4)	19(4)	O(79)	597(3)	3345(10)	3407(4)	18(4)
O(6)	100(3)	5652(10)	4709(4)	20(4)	O(80)	22(3)	4401(10)	4141(4)	21(4)
O(7)	1328(3)	2788(10)	6451(5)	23(4)	O(81)	239(3)	4473(11)	3523(5)	26(5)
O(8)	1407(3)	4315(10)	6179(5)	24(4)	O(82)	467(3)	4365(10)	2894(5)	26(5)
O(9)	1330(3)	3096(10)	5680(4)	16(4)	O(83)	1177(3)	2306(10)	4371(5)	25(5)
O(10)	891(3)	2723(10)	5995(5)	23(4)	O(84)	1162(3)	4502(10)	4360(4)	19(4)
O(11)	411(3)	2659(11)	5659(5)	26(5)	O(85)	1284(3)	3463(9)	4866(4)	14(4)
O(12)	487(3)	4159(9)	5368(4)	12(4)	O(86)	1503(3)	3473(9)	4266(4)	14(4)
O(13)	831(3)	3011(10)	5252(5)	23(4)	O(87)	764(3)	5778(9)	4516(4)	13(4)
O(14)	671(3)	6561(10)	6440(5)	23(4)	O(88)	432(3)	6767(10)	4608(4)	21(4)
O(15)	964(3)	5709(10)	5524(5)	24(4)	O(89)	542(3)	5757(9)	5106(4)	15(4)
O(16)	642(3)	6855(10)	5673(4)	19(4)	O(90)	824(3)	5684(11)	2731(5)	30(5)
O(17)	1107(3)	6798(11)	6029(5)	30(5)	O(91)	947(3)	6745(10)	3248(5)	25(5)
O(18)	1793(3)	3243(10)	6079(5)	25(5)	O(92)	1062(3)	5756(10)	3748(4)	16(4)
O(19)	1363(3)	4531(10)	5404(5)	21(4)	O(93)	1272(3)	5735(10)	3135(4)	20(4)
O(20)	1738(3)	3555(10)	5324(4)	19(4)	O(94)	1134(3)	6831(10)	4326(4)	16(4)
O(21)	1783(3)	4777(11)	5805(5)	27(5)	O(95)	1379(3)	6808(10)	3647(4)	21(4)
O(22)	373(3)	3023(10)	4823(5)	23(4)	O(96)	877(3)	6827(10)	4992(4)	17(4)
O(23)	895(3)	4540(9)	4989(4)	13(4)	O(97)	1596(3)	4565(10)	4745(4)	20(4)
O(24)	813(3)	3374(9)	4490(4)	15(4)	O(98)	1511(3)	5718(11)	4212(5)	26(5)
O(25)	459(3)	4507(10)	4603(5)	21(4)	O(99)	1247(3)	5701(10)	4885(4)	18(4)

Table 7 (Continued)

	x	*y*	*z*	*U*(eq)[a]		*x*	*y*	*z*	*U*(eq)[a]
O(100)	356(4)	8155(12)	5846(5)	36(5)	O(137)	3075(4)	3783(14)	5791(6)	52(6)
O(101)	997(3)	7951(11)	5503(5)	27(5)	C(1)	878(6)	3377(18)	6771(8)	34(8)
O(102)	713(3)	9077(11)	5615(5)	29(5)	C(2)	467(5)	3266(17)	6420(8)	32(8)
O(103)	820(3)	8006(10)	6140(5)	26(5)	C(3)	793(5)	2325(16)	6031(7)	27(7)
O(104)	1362(4)	8913(12)	5234(5)	38(5)	C(4)	623(6)	2273(18)	6890(8)	37(8)
O(105)	1189(4)	8930(12)	5926(5)	39(5)	C(5)	696(5)	2282(17)	2895(8)	30(7)
O(106)	1073(4)	10050(13)	5434(6)	45(6)	C(6)	2047(6)	2282(17)	2895(8)	30(7)
O(107)	1477(4)	7707(14)	5821(7)	56(7)	C(7)	1953(6)	3285(18)	2395(8)	37(8)
O(108)	1295(4)	7950(14)	6484(6)	53(6)	C(8)	2358(6)	3295(18)	2768(8)	34(8)
O(109)	2140(4)	2625(11)	5255(5)	31(5)	C(9)	2285(7)	2289(20)	2320(9)	48(9)
O(110)	2032(3)	4770(10)	5142(5)	25(5)	C(10)	2157(5)	2814(17)	2598(8)	29(7)
O(111)	2176(3)	3909(10)	5703(5)	23(4)	C(11)	122(6)	9189(18)	2970(8)	37(8)
O(112)	2414(3)	3899(10)	5069(5)	24(4)	C(12)	204(6)	10232(18)	3449(8)	36(8)
O(113)	1641(3)	2412(10)	4793(5)	22(4)	C(13)	−116(5)	9204(17)	3544(8)	29(7)
O(114)	2232(4)	5160(12)	6168(6)	40(6)	C(14)	−189(7)	10230(21)	3064(10)	53(10)
O(115)	2323(4)	6016(13)	4895(6)	44(6)	C(15)	3(6)	9686(18)	3262(8)	35(8)
O(116)	2706(4)	5119(13)	4907(6)	44(6)	C(16)	71(6)	3909(17)	3377(8)	34(8)
O(117)	1581(4)	8145(12)	2517(5)	35(5)	C(17)	179(6)	2913(18)	3872(8)	37(8)
O(118)	1739(3)	7933(10)	3566(3)	26(5)	C(18)	383(6)	2894(18)	3270(8)	37(8)
O(119)	1991(4)	7979(11)	2999(5)	30(5)	C(19)	−53(7)	2554(21)	3302(9)	50(10)
O(120)	1648(3)	9053(11)	3127(5)	29(5)	C(20)	157(6)	3092(18)	3462(8)	36(8)
O(121)	1779(4)	8894(12)	4188(5)	39(5)	C(21)	681(6)	9596(19)	5913(8)	39(8)
O(122)	1740(4)	10065(12)	3707(6)	41(6)	C(22)	1097(7)	9449(22)	6198(10)	53(10)
O(123)	2060(4)	8934(12)	3590(5)	37(5)	C(23)	774(6)	8601(16)	6393(8)	30(7)
O(124)	2162(5)	7712(14)	4052(7)	58(7)	C(24)	767(7)	10005(21)	6538(9)	51(10)
O(125)	2423(4)	7918(13)	3447(6)	50(6)	C(25)	834(6)	9389(20)	6261(9)	45(9)
O(126)	1167(3)	6854(11)	2594(5)	31(5)	C(26)	2406(5)	3653(16)	5879(7)	25(7)
O(127)	516(3)	3799(10)	6130(4)	19(4)	C(27)	2619(6)	3631(18)	5292(8)	33(8)
O(128)	184(3)	6836(10)	5244(5)	22(4)	C(28)	2638(6)	4777(17)	5698(8)	32(8)
O(129)	2438(4)	5148(11)	5508(5)	33(5)	C(29)	2843(6)	3597(19)	5912(8)	38(8)
O(130)	2035(4)	6047(12)	5628(5)	35(5)	C(30)	2625(6)	3935(18)	5695(8)	34(8)
O(131)	508(4)	2652(12)	7190(6)	42(6)	C(31)	2107(7)	8603(20)	2808(10)	53(10)
O(132)	2104(6)	1728(20)	2157(9)	98(10)	C(32)	1798(7)	9557(21)	2905(10)	52(10)
O(133)	−91(13)	10749(42)	2806(19)	136(24)	C(33)	2173(7)	9447(21)	3332(9)	51(10)
O(134)	−97(8)	2596(25)	2917(12)	137(15)	C(34)	2207(7)	9934(23)	2712(10)	59(11)
O(135)	848(7)	9803(21)	6904(10)	109(12)	C(35)	2064(6)	9372(20)	2942(9)	42(9)
O(136)	2110(8)	9972(26)	2359(12)	138(15)					

[a] Equivalent isotropic *U* defined as one-third of the trace of the orthogonalized $\mathbf{U}_{ij}$ tensor.

rotating-anode diffractometer operating at 18 kW, employing Cu Kα radiation ($\lambda = 1.541\,78$ Å). In an effort to reduce data collection times and to improve data quality by collecting all data and averaging the intensities, data for **6**·10H_2O were collected on the Siemens SMART system equipped with a 2D detector using a CCD chip coupled to fiberoptic tape. This resulted in considerable improvement in data collection time and reflection to parameter ratio in comparison to those of the conventional systems: 12 h *vs* 10 days and 12.3:1 *vs* 7.6:1, respectively.

Crystal stability was monitored in all cases using three standard reflections, monitored every 250 reflections. In no case was significant crystal decomposition observed during the course of data collection.

For each of the four studies, data were corrected for Lorentz, polarization, and absorption effects in the usual fashion. Structures **1** and **2** were solved by Patterson techniques, while **3**−**6** were solved by direct methods; all were refined by full-matrix least-squares using the SHELXS-86, SHELXTL, or TEXSAN program packages.[27−30] In all cases, refinement of the anions proceeded routinely, and no anomalies in temperature factors or unusual excursions of electron density in the final Fourier maps were observed.

Structures **3**−**6** exhibited varying degrees of disorder in the organic cations and the water molecules of crystallization. In the cases of **3**·15H_2O and **5**·25H_2O·0.5$C(CH_2OH)_4$ in particular, several water sites were considerably "smeared" and the degree of hydration is only approximate. However, in all cases, the number of water molecules of crystallization determined from the structural analysis is in good agreement with results from the thermal gravimetric analyses.

Magnetic Studies. The magnetic susceptibility data were recorded on a 59.51 mg polycrystalline sample of compound **5** over the 2−300 K temperature region using a Quantum Design MPMS-5S SQUID susceptometer. Measurement and calibration techniques have been reported elsewhere.[31] The temperature-dependent magnetic data were measured at a magnetic field of 1000 G. Room-temperature susceptibilities of **1** and **2** were measured on 48.32 and 55.97 mg samples, respectively, by the Faraday technique employing a Kahn electrobalance.

Results and Discussion

Syntheses and Physical Properties. (a) The Mixed-Valence Mo(V)/Mo(VI) Polyoxide Clusters: $(NH_4)_7[NaMo_{16}(OH)_{12}O_{40}O]\cdot 4H_2O$ (1·4H_2O) and $(Me_3NH)_4K_2[H_2Mo_{16}(OH)_{12}O_{40}]\cdot 8H_2O$ (2·8H_2O). There are no general synthetic routes for preparing cluster compounds of predictable features. Conventional synthetic methods involve hydrolysis and fragment condensation reactions or "self-assembly" of complex products from simpler molecular precursors in solution. Under these conditions, molecular species present at the initial stages of hydrolysis/condensation processes may be isolated and the structures and properties of these species may be related to those of larger aggregates or even solids formed under more forcing

(27) Calabrese, J. C. PHASE-Patterson Heavy Atom Solution Extractor. Ph.D. Thesis, University of Wisconsin−Madison, 1972. Beurskens, P. T. DIRDIF−Direct Methods for Difference Structures and Automatic Procedure for Phase Extraction and Refinement of Difference Structure Factors. Technical Report 1984/1; Crystallographic Laboratory: Toernooiveld, 6252 Ed Nijmegen, The Netherlands, 1984.
(28) Cromer, D. T.; Waber, J. T. *International Tables for X-ray Crystallography*; Kynoch Press: Birmingham, England, 1974; Vol. IV, Table 2.2A.
(29) Ibers, J. A.; Hamilton, W. C. *Acta Crystallogr.* **1964**, *17*, 781.
(30) Cromer, D. T. *International Tables for X-ray Crystallography*; Kynoch Press: Birmingham, England, 1974; Vol. IV, Table 2.3.1.
(31) O'Connor, C. J. *Prog. Inorg. Chem.* **1982**, *29*, 203.
(32) Mallouk, T. E.; Lee, H. *J. Chem. Educ.* **1990**, *67*, 829.

Table 8. Atomic Positional Parameters ($\times 10^4$) and Isotropic Temperature Factors (Å^2 $\times$ 10^3) for the Molecular Anion and the Sodium Cations of $Na_9[(MoO_3)H_{14}Mo_{42}O_{109}\{(OCH_2)_3CCH_2OH\}_7]\cdot 0.5C(CH_2OH)_4\cdot 25H_2O$ (**5**$\cdot 0.5C(CH_2OH)_4\cdot 25H_2O$)

	x	*y*	*z*	*U*(eq)[a]		*x*	*y*	*z*	*U*(eq)[a]
Mo(1)	2602(3)	6859(3)	4008(2)	17(2)	O(23)	5515(18)	5273(15)	3923(11)	11(7)
Mo(2)	2266(3)	6600(3)	2974(2)	18(2)	O(24)	4646(20)	5846(18)	3430(13)	20(9)
Mo(3)	4541(3)	7875(3)	4773(2)	18(2)	O(25)	3956(19)	4492(16)	3303(12)	13(8)
Mo(4)	5764(3)	8436(2)	4359(2)	15(2)	O(26)	3232(26)	10026(22)	3754(16)	48(12)
Mo(5)	3782(3)	6137(2)	4582(2)	14(2)	O(27)	4517(23)	9423(20)	3757(14)	34(11)
Mo(6)	4372(3)	5293(2)	4028(2)	14(2)	O(28)	2913(22)	8629(19)	3110(14)	30(10)
Mo(7)	3657(3)	9584(3)	3343(2)	21(2)	O(29)	4268(21)	9335(18)	2645(13)	23(9)
Mo(8)	3669(3)	8583(3)	3734(2)	19(2)	O(30)	2909(20)	9660(17)	2668(12)	17(9)
Mo(9)	3243(3)	9277(3)	1959(2)	20(2)	O(31)	4587(21)	10538(18)	3343(13)	22(9)
Mo(10)	2939(3)	8033(3)	1334(2)	18(2)	O(32)	3207(20)	8845(17)	4245(12)	17(9)
Mo(11)	5303(3)	10359(3)	2784(2)	21(2)	O(33)	4232(19)	8047(16)	3128(12)	10(8)
Mo(12)	6541(3)	9935(3)	2773(2)	20(2)	O(34)	2623(21)	9542(18)	1586(13)	24(9)
Mo(13)	1047(3)	3663(3)	2690(2)	21(2)	O(35)	2513(20)	8366(17)	1949(12)	17(9)
Mo(14)	2031(3)	4881(3)	3355(2)	19(2)	O(36)	3896(21)	8956(18)	1523(13)	21(9)
Mo(15)	1867(3)	2535(3)	1933(2)	22(2)	O(37)	4245(20)	10336(17)	2224(12)	17(9)
Mo(16)	3465(3)	2936(3)	2028(2)	21(2)	O(38)	2240(22)	8048(19)	797(14)	30(10)
Mo(17)	686(3)	3360(3)	1307(2)	23(2)	O(39)	3808(18)	7793(16)	1990(12)	8(8)
Mo(18)	1369(3)	4347(3)	922(2)	21(2)	O(40)	3655(18)	7566(16)	960(12)	9(8)
Mo(19)	7658(3)	7127(3)	5346(2)	17(2)	O(41)	2286(20)	6973(17)	1342(12)	18(9)
Mo(20)	6155(3)	7059(3)	5004(2)	17(2)	O(42)	5803(19)	11252(17)	2864(12)	15(8)
Mo(21)	9233(3)	7793(3)	4705(2)	22(2)	O(43)	5596(20)	9818(17)	2205(12)	18(9)
Mo(22)	8930(3)	8251(3)	3921(2)	21(2)	O(44)	5978(21)	10174(18)	3329(13)	22(9)
Mo(23)	8442(3)	5970(3)	4600(2)	22(2)	O(45)	7320(21)	10731(18)	2850(13)	23(9)
Mo(24)	7535(3)	5053(3)	3691(2)	21(2)	O(46)	5604(21)	8765(18)	2707(13)	25(9)
Mo(25)	3986(3)	4980(3)	2724(2)	14(2)	O(47)	6830(20)	9282(17)	2189(12)	18(9)
Mo(26)	3082(3)	5565(3)	2259(2)	15(2)	O(48)	7257(19)	9578(16)	3294(12)	13(8)
Mo(27)	3832(3)	7320(3)	2440(2)	17(2)	O(49)	326(22)	3442(19)	3011(14)	30(10)
Mo(28)	5348(3)	8105(3)	3043(2)	16(2)	O(50)	2103(20)	3958(17)	3190(12)	18(9)
Mo(29)	6478(3)	7343(3)	3625(2)	17(2)	O(51)	1271(20)	4646(17)	2700(13)	19(9)
Mo(30)	5886(3)	5971(3)	3486(2)	16(2)	O(52)	1745(21)	3591(18)	2028(13)	22(9)
Mo(31)	1715(3)	6093(2)	705(2)	15(2)	O(53)	1045(19)	2605(16)	2440(12)	10(8)
Mo(32)	1924(3)	6316(3)	1738(2)	15(2)	O(54)	138(23)	3320(20)	1964(15)	37(11)
Mo(33)	2766(3)	5056(3)	134(2)	22(2)	O(55)	1495(21)	4921(18)	3797(13)	22(9)
Mo(34)	3584(3)	6907(3)	361(2)	19(2)	O(56)	2929(18)	5105(15)	2799(11)	15(7)
Mo(35)	8390(3)	9550(3)	3356(2)	23(2)	O(57)	1588(19)	1646(17)	1786(12)	14(8)
Mo(36)	7217(3)	9068(3)	3835(2)	19(2)	O(58)	755(22)	2357(19)	1318(14)	28(10)
Mo(37)	8788(3)	8191(3)	2548(2)	28(3)	O(59)	2564(20)	2841(18)	1454(13)	21(9)
Mo(38)	7668(3)	9063(3)	1986(2)	31(3)	O(60)	2794(19)	2954(16)	2555(12)	12(8)
Mo(39)	5715(3)	3474(2)	2780(2)	17(2)	O(61)	3521(21)	2137(18)	1887(13)	22(9)
Mo(40)	5080(3)	4275(3)	3363(2)	18(2)	O(62)	3607(21)	4189(18)	2243(13)	25(10)
Mo(41)	5224(3)	3375(3)	1425(2)	25(2)	O(63)	4243(20)	3373(18)	1572(13)	19(9)
Mo(42)	7249(3)	4450(3)	2257(2)	25(2)	O(64)	4587(19)	3533(16)	2692(12)	12(8)
Mo(43)	5369(4)	6335(3)	2119(2)	40(3)	O(65)	−255(22)	2904(19)	845(14)	28(10)
Na(1)	3898(13)	4866(11)	5290(8)	28(6)	O(66)	806(18)	4342(15)	1492(11)	24(7)
Na(2)	9488(13)	4893(11)	7819(8)	28(6)	O(67)	1540(24)	3449(20)	931(15)	38(11)
Na(3)	3024(13)	3435(11)	3482(8)	29(6)	O(68)	600(21)	4119(18)	405(13)	23(9)
Na(4)	8319(14)	2169(12)	7550(9)	38(6)	O(69)	2578(20)	4872(17)	1687(12)	18(9)
Na(5)	2098(14)	1068(12)	4909(9)	35(6)	O(70)	2365(23)	4573(20)	596(15)	36(11)
Na(6)	1710(19)	3543(16)	6808(12)	75(9)	O(71)	1684(20)	5463(17)	1143(12)	16(9)
Na(7)	9844(33)	3371(28)	5989(20)	124(18)	O(72)	7730(20)	7307(17)	5995(13)	19(9)
Na(8)	8358(30)	962(26)	4995(19)	112(16)	O(73)	6606(18)	6334(16)	4989(12)	8(8)
Na(9)	4709(30)	4002(25)	9261(19)	155(18)	O(74)	7246(22)	7806(19)	5122(14)	27(10)
O(1)	1716(20)	6888(17)	4095(12)	19(9)	O(75)	7994(19)	6830(16)	4564(12)	12(8)
O(2)	2917(22)	7463(19)	3556(14)	27(10)	O(76)	8913(19)	7866(16)	5445(12)	12(8)
O(3)	2244(20)	5944(17)	3404(12)	17(9)	O(77)	8331(20)	6422(17)	5370(13)	19(9)
O(4)	3815(19)	6854(16)	4175(12)	12(8)	O(78)	5921(22)	7273(19)	5583(14)	29(10)
O(5)	3263(20)	7762(18)	4679(13)	19(9)	O(79)	6187(20)	6811(17)	4138(12)	16(9)
O(6)	2621(19)	6269(16)	4538(12)	11(8)	O(80)	10281(23)	8358(20)	4988(15)	38(11)
O(7)	1270(20)	6571(17)	2867(13)	19(9)	O(81)	9123(21)	7405(19)	3958(13)	26(9)
O(8)	2564(20)	7169(17)	2451(12)	17(9)	O(82)	8619(21)	8385(18)	4570(13)	22(9)
O(9)	3520(20)	6546(17)	2904(12)	17(9)	O(83)	9567(19)	6958(17)	4831(12)	15(8)
O(10)	2020(19)	5778(16)	2314(12)	12(8)	O(84)	9909(21)	8902(18)	4049(13)	22(9)
O(11)	4834(22)	8560(19)	5376(14)	28(10)	O(85)	7499(19)	7404(16)	3645(12)	12(8)
O(12)	5600(18)	7680(15)	4725(11)	14(7)	O(86)	8710(22)	7911(19)	3122(14)	26(10)
O(13)	4577(20)	8380(17)	4217(12)	17(9)	O(87)	8229(18)	8884(15)	3744(11)	25(7)
O(14)	4300(19)	7186(16)	5181(12)	13(8)	O(88)	8993(22)	5530(19)	4832(14)	32(10)
O(15)	6255(23)	9186(20)	4870(14)	33(10)	O(89)	8564(21)	5922(18)	3908(13)	23(9)
O(16)	6849(18)	8305(16)	4230(12)	8(8)	O(90)	7216(19)	5320(17)	4364(12)	15(9)
O(17)	5342(19)	7506(16)	3627(12)	10(8)	O(91)	7874(23)	4427(20)	3737(14)	34(10)
O(18)	5957(18)	8912(16)	3776(11)	7(8)	O(92)	6837(17)	5867(15)	3539(11)	10(7)
O(19)	3587(18)	5739(16)	5054(12)	9(8)	O(93)	7532(18)	5061(16)	2930(11)	8(8)
O(20)	3277(19)	5342(16)	3916(12)	10(8)	O(94)	6267(19)	4373(16)	3342(12)	11(8)
O(21)	4907(21)	6202(18)	4574(13)	22(9)	O(95)	4267(19)	5674(17)	2350(12)	13(8)
O(22)	4316(22)	4782(19)	4435(14)	32(10)	O(96)	3223(20)	6327(17)	1881(12)	18(9)

Table 8 (Continued)

	x	*y*	*z*	*U*(eq)[a]		*x*	*y*	*z*	*U*(eq)[a]
O(97)	4913(18)	7177(16)	2476(11)	8(8)	O(137)	9267(26)	3110(23)	3645(17)	53(13)
O(98)	6533(21)	8045(18)	3164(13)	26(10)	O(138)	−872(21)	4886(18)	1635(13)	22(9)
O(99)	5856(19)	6520(16)	2944(12)	9(8)	O(139)	1195(33)	1170(29)	3172(21)	84(17)
O(100)	5204(19)	5004(17)	2862(12)	14(8)	O(140)	6419(26)	1347(22)	1370(16)	47(12)
O(101)	768(21)	6087(18)	555(13)	22(9)	C(1)	2950(32)	7142(28)	5399(20)	21(14)
O(102)	3001(21)	6057(18)	741(13)	25(10)	C(2)	2919(35)	7763(30)	5177(22)	30(15)
O(103)	1576(20)	5274(17)	82(12)	16(9)	C(3)	2323(30)	6366(26)	4932(19)	15(13)
O(104)	2262(19)	6694(17)	251(12)	14(8)	C(4)	3885(45)	7213(39)	5626(28)	63(22)
O(105)	972(19)	6274(16)	1734(12)	12(8)	C(5)	2551(37)	7236(33)	5893(23)	36(17)
O(106)	3789(22)	5200(19)	267(14)	27(10)	C(6)	3615(33)	10957(29)	2857(21)	24(14)
O(107)	2314(22)	4381(19)	−498(14)	32(10)	C(7)	2817(34)	10385(29)	2751(21)	26(15)
O(108)	3027(19)	5895(17)	−213(12)	15(8)	C(8)	4264(37)	11135(32)	3347(23)	37(17)
O(109)	4546(21)	6870(19)	497(13)	32(10)	C(9)	3959(32)	10909(27)	2301(20)	19(14)
O(110)	3623(22)	7315(19)	−126(14)	32(10)	C(10)	3394(38)	11597(33)	2851(24)	39(17)
O(111)	9007(24)	10316(21)	3799(15)	42(12)	C(11)	−345(30)	1982(26)	1766(19)	14(13)
O(112)	7767(20)	8556(17)	2642(13)	18(9)	C(12)	250(41)	2018(35)	2280(26)	50(19)
O(113)	9375(19)	9338(17)	3191(12)	13(8)	C(13)	−571(28)	2605(25)	1862(18)	18(12)
O(114)	8439(21)	9900(18)	2729(13)	26(10)	C(14)	−12(33)	1843(29)	1325(21)	26(15)
O(115)	7626(22)	9762(19)	4430(14)	27(10)	C(15)	8732(39)	1324(34)	1656(24)	45(18)
O(116)	9796(21)	8265(18)	2493(14)	26(10)	C(16)	9753(33)	7247(28)	5785(20)	22(14)
O(117)	8164(29)	7466(25)	2002(18)	63(14)	C(17)	9574(32)	7915(28)	5881(20)	22(14)
O(118)	8840(20)	8967(17)	2080(12)	18(9)	C(18)	9001(32)	6622(27)	5800(20)	20(14)
O(119)	8023(21)	9636(18)	1633(13)	23(9)	C(19)	10108(38)	7047(33)	5294(24)	40(17)
O(120)	7143(27)	8237(24)	1507(17)	58(13)	C(20)	10543(32)	7519(28)	6348(20)	18(13)
O(121)	5667(22)	2868(19)	3095(14)	32(10)	C(21)	1634(34)	5861(30)	−626(21)	26(15)
O(122)	5935(23)	4218(20)	2249(14)	35(11)	C(22)	1090(30)	5154(26)	−453(19)	14(13)
O(123)	5294(21)	2745(18)	2012(13)	21(9)	C(23)	1680(35)	6541(31)	−268(22)	31(16)
O(124)	6838(21)	3598(18)	2671(13)	23(9)	C(24)	2433(32)	5867(28)	−684(20)	21(14)
O(125)	4881(21)	3791(18)	3784(13)	25(9)	C(25)	−1063(43)	4268(37)	1200(27)	57(21)
O(126)	5418(26)	4009(23)	1125(16)	52(13)	C(26)	9908(37)	10041(32)	2682(23)	34(16)
O(127)	4959(22)	2586(19)	891(14)	29(10)	C(27)	10090(31)	9797(27)	3117(19)	17(13)
O(128)	6472(26)	3468(23)	1590(16)	50(12)	C(28)	9292(31)	10448(27)	2736(19)	16(13)
O(129)	8158(22)	4284(19)	2218(14)	30(10)	C(29)	9653(37)	9462(32)	2208(23)	37(17)
O(130)	2748(20)	4992(17)	8116(12)	16(9)	C(30)	10773(40)	10527(34)	2661(25)	46(18)
O(131)	5643(24)	5569(21)	1978(15)	42(12)	C(31)	6617(33)	2436(29)	1941(21)	23(14)
O(132)	6305(22)	7066(19)	2149(14)	29(10)	C(32)	5606(31)	2185(27)	1889(20)	19(13)
O(133)	10702(126)	6556(113)	4854(82)	181(28)	C(33)	7203(26)	3102(23)	2538(16)	21(11)
O(134)	7135(33)	2063(29)	3815(21)	86(18)	C(34)	6748(36)	2880(31)	1516(22)	31(16)
O(135)	2977(23)	1788(20)	3327(14)	34(11)	C(35)	6969(41)	1863(35)	1870(26)	49(19)
O(136)	4719(27)	6204(23)	1501(17)	58(14)					

[a] Equivalent isotropic *U* defined as one-third of the trace of the orthogonalized $\mathbf{U}_{ij}$ tensor.

conditions. Furthermore, such soluble building blocks may be induced to aggregate into supramolecular materials and conceivably designer solids.[32]

The molecular building block approach is quite attractive since it offers not only a conceptional framework for the design of topologically controlled materials but also several synthetic advantages, namely, (i) the extensive chemistry of coordination complexes and clusters which provide precursors for the synthesis of more complex assemblies, (ii) the functional group reactivity and molecular symmetry of the starting materials which may be exploited in the synthesis of the product cluster, (iii) the good solubility of molecular starting materials affording low reaction temperatures, and thus favoring the kinetic trapping of interesting metastable structures, and (iv) reactions which proceed by transformation of some of the functional groups of the organic and inorganic starting materials while retaining the covalent bonding relationships between most of the atoms, a feature which tends to direct the assembly of the more complex frameworks.

While the detailed principles underlying polyanion accretion remain elusive,[33,34] fragment condensation processes have been invoked and have been demonstrated in the sequential synthesis under conventional conditions of higher oligomers, such as $[Mo_3O_6(OR)\{(OCH_2)_3CR\}_2]^-$, $[Mo_4O_8(OR)_2\{(OCH_2)_3CR\}_2]$, and $[H_2Mo_8O_{20}(OR)_4\{(OCH_2)_3CR\}_2]$, from $[Mo_2O_4\{(OCH_2)_3CR\}_2]^{2-}$.[35−38] However, attempts to exploit the trinuclear species $[Mo_3O_6(OR)\{(OCH_2)_3CR\}_2]^-$ in the preparation of superclusters proved unsuccessful, whether in the presence of excess oxomolybdenum(VI) or upon addition of molybdenum(V)-containing solutions, both in neutral and acidic solutions and in a variety of organic solvents.

While fragment condensation under conventional conditions failed to produce large oligomers of the Mo−O−alkoxide family, hydrothermal synthesis provided a low-temperature pathway to a variety of superclusters of this class of materials and also to two novel mixed-valence Mo(V)/Mo(VI) polyanions which serve as the structural core for the series of compounds.

Hydrothermal reactions, typically carried out in a temperature range of 140−260 °C under autogenous pressure, exploit the self-assembly of the product from soluble precursors.[39] The reduced viscosity of the solvent under these conditions results in enhanced rates of solvent extraction of solids and crystal growth from solution. Since differential solubility problems are minimized, a variety of simple precursors may be introduced, as well as a number of organic and/or inorganic structure-directing (templating) agents from which those of appropriate

(33) Kepert, D. L. *Inorg. Chem.* **1969**, *8*, 1556.
(34) Tytko, K. H.; Glemser, O. *Adv. Inorg. Chem. Radiochem.* **1976**, *19*, 239.
(35) Ma., L.; Liu, S.; Zubieta, J. *Inorg. Chem.* **1989**, *28*, 175.
(36) Liu, S.; Shaikh, S. N.; Zubieta, J. *Inorg. Chem.* **1987**, *26*, 4305.
(37) McKee, V.; Wilkins, C. J. *J. Chem. Soc., Dalton Trans.* **1987**, 523.
(38) Gumaer, E.; Lettko, K.; Ma, L.; Macherone, D.; Zubieta, J. *Inorg. Chim. Acta* **1991**, *179*, 47.
(39) Rabenau, A. *Angew. Chem., Int. Ed. Engl.* **1985**, *24*, 1026.

Table 9. Atomic Positional Parameters ($\times 10^4$) and Isotropic Temperature Factors ($Å^2 \times 10^3$) for the Molecular Anion and the Sodium Cations of $(Me_4N)(Et_2NH_2)(H_3O)_2Na_6[(MoO_3)H_{13}Mo_{42}O_{109}\{(OCH_2)_3CCH_3\}_7]\cdot 10H_2O$ (**6**·$10H_2O$)

	x	*y*	*z*	*U*(eq)[a]		*x*	*y*	*z*	*U*(eq)[a]
Mo(1)	7390(1)	3835(1)	−678(1)	48(1)	O(36)	2401(8)	2399(3)	2500	42(5)
Mo(2)	6033(1)	3810(1)	−330(1)	42(1)	O(37)	2736(7)	2944(2)	627(4)	51(4)
Mo(3)	8796(1)	3450(1)	88(1)	44(1)	O(38)	4282(5)	3111(2)	1851(4)	34(3)
Mo(4)	8486(1)	3146(1)	988(1)	37(1)	O(39)	4223(6)	3135(2)	674(3)	34(3)
Mo(5)	8749(1)	4249(1)	97(1)	48(1)	O(40)	3177(6)	3442(2)	1340(4)	44(4)
Mo(6)	8395(1)	4541(1)	1001(1)	41(1)	O(41)	9809(8)	2839(3)	2500	46(6)
Mo(7)	3014(1)	2513(1)	1743(1)	41(1)	O(42)	7724(8)	2781(3)	2500	29(5)
Mo(8)	3321(1)	2990(1)	1176(1)	39(1)	O(43)	8753(6)	2546(2)	1889(4)	39(4)
Mo(9)	4415(1)	2117(1)	2500	35(1)	O(44)	9776(8)	3528(3)	2500	44(6)
Mo(10)	5761(1)	2317(1)	2500	30(1)	O(45)	8649(6)	3831(2)	1942(4)	35(3)
Mo(11)	7604(1)	2495(1)	1787(1)	32(1)	O(46)	7656(8)	3536(3)	2500	33(5)
Mo(12)	6556(1)	2765(1)	1201(1)	30(1)	O(47)	7746(6)	2201(2)	1343(4)	37(4)
Mo(13)	8876(1)	2890(1)	2500	36(1)	O(48)	7689(8)	2206(3)	2500	32(5)
Mo(14)	8852(1)	3477(1)	2500	36(1)	O(49)	6520(6)	2516(2)	665(4)	38(4)
Mo(15)	5229(1)	3137(1)	1942(1)	26(1)	O(50)	6436(5)	3147(2)	1822(3)	28(3)
Mo(16)	6515(1)	3530(1)	1220(1)	30(1)	O(51)	6427(5)	3147(2)	698(3)	31(3)
Mo(17)	7512(1)	3833(1)	1793(1)	30(1)	O(52)	5431(5)	2845(2)	1254(3)	30(3)
Mo(18)	4258(1)	3420(1)	22(1)	41(1)	O(53)	5343(8)	3456(3)	2500	28(5)
Mo(19)	5309(1)	3115(1)	542(1)	31(1)	O(54)	6431(5)	3796(2)	1883(3)	30(3)
Mo(20)	4398(1)	4206(1)	208(1)	54(1)	O(55)	7574(8)	4112(3)	2500	30(5)
Mo(21)	3052(1)	3798(1)	976(1)	51(1)	O(56)	4121(7)	3192(3)	−553(4)	53(4)
Mo(22)	8801(1)	4189(1)	2500	36(1)	O(57)	4240(6)	3782(2)	721(4)	43(4)
Mo(23)	8669(1)	4780(1)	2500	37(1)	O(58)	4214(6)	3827(2)	−397(4)	43(4)
Mo(24)	7078(1)	5030(1)	3255(1)	42(1)	O(59)	3166(6)	3507(2)	204(4)	48(4)
Mo(25)	5529(2)	3955(1)	2500	53(1)	O(60)	5358(6)	2832(2)	55(4)	34(3)
Na(1)	9746(4)	3845(2)	1388(3)	56(3)	O(61)	5397(5)	3438(2)	1279(3)	32(3)
Na(2)	4876(4)	2325(2)	909(2)	51(2)	O(62)	4408(8)	4423(3)	826(5)	73(5)
Na(3)	7036(4)	2029(2)	309(3)	58(3)	O(63)	4208(8)	4459(3)	−324(5)	78(6)
O(1)	7259(8)	3849(3)	−1390(4)	63(5)	O(64)	3228(7)	4053(3)	1512(5)	70(5)
O(2)	6784(6)	3507(2)	−400(4)	44(4)	O(65)	2132(7)	3822(3)	842(5)	73(5)
O(3)	6745(6)	4135(2)	−350(4)	45(4)	O(66)	3258(6)	4117(3)	323(4)	52(4)
O(4)	8004(6)	3838(2)	177(4)	43(4)	O(67)	9737(9)	4182(4)	2500	55(6)
O(5)	8270(7)	3530(3)	−723(4)	54(4)	O(68)	9578(9)	4896(3)	2500	46(6)
O(6)	8250(7)	4169(3)	−717(4)	54(5)	O(69)	7397(8)	4738(3)	2500	37(5)
O(7)	5608(7)	3805(2)	−968(4)	53(4)	O(70)	8300(6)	5089(2)	3089(4)	34(3)
O(8)	6453(6)	3768(2)	632(4)	36(4)	O(71)	6150(6)	4939(3)	1822(5)	54(4)
O(9)	5371(6)	4103(2)	112(4)	45(4)	O(72)	7094(6)	5353(2)	1331(4)	51(4)
O(10)	5360(6)	3476(2)	48(4)	35(4)	O(73)	7061(8)	5292(3)	2500	38(5)
O(11)	9459(7)	3236(3)	−207(5)	60(5)	O(74)	4900(11)	3973(4)	1919(7)	75(8)
O(12)	7972(6)	3188(2)	261(4)	37(4)	O(75)	5982(18)	4308(6)	2500	92(14)
O(13)	9085(6)	3507(2)	881(4)	42(4)	C(1)	9301(11)	3861(4)	−1153(7)	59(5)
O(14)	9398(6)	3857(2)	−92(4)	49(4)	C(2)	8828(11)	3566(4)	−1185(8)	63(5)
O(15)	9060(6)	2858(2)	870(4)	46(4)	C(3)	8806(11)	4139(4)	−1181(8)	71(6)
O(16)	7603(6)	3474(2)	1296(3)	33(3)	C(4)	9792(11)	3864(4)	−624(7)	65(5)
O(17)	8729(5)	3182(2)	1868(4)	36(4)	C(5)	9810(12)	3875(5)	−1687(8)	78(6)
O(18)	7637(6)	2846(2)	1263(4)	34(3)	C(6)	2552(14)	1851(5)	2500	47(6)
O(19)	9369(7)	4490(3)	−212(4)	63(5)	C(7)	3021(9)	1844(3)	1973(6)	42(4)
O(20)	7871(6)	4476(2)	287(4)	41(4)	C(8)	2026(13)	2129(5)	2500	49(6)
O(21)	9064(6)	4202(2)	879(4)	42(4)	C(9)	2086(14)	1591(5)	2500	61(7)
O(22)	8942(7)	4844(2)	901(4)	50(4)	C(10)	9050(14)	2100(5)	2500	43(6)
O(23)	7609(6)	4122(2)	1305(4)	37(4)	C(11)	9226(10)	2278(3)	1956(6)	47(4)
O(24)	7421(6)	4733(2)	1276(4)	42(4)	C(12)	8241(12)	1977(5)	2500	46(6)
O(25)	8616(6)	4484(2)	1874(4)	39(4)	C(13)	9593(14)	1849(5)	2500	65(8)
O(26)	4550(10)	1738(3)	2500	50(6)	C(14)	2884(11)	3861(4)	−580(8)	61(5)
O(27)	5031(6)	2290(2)	1889(3)	35(3)	C(15)	3646(10)	3861(4)	−835(7)	58(5)
O(28)	3786(8)	2565(3)	2500	36(5)	C(16)	2668(10)	3565(4)	−291(7)	51(5)
O(29)	3524(6)	2085(2)	1893(4)	40(4)	C(17)	2743(10)	4128(4)	−175(7)	58(5)
O(30)	6181(8)	1983(3)	2500	32(5)	C(18)	2309(12)	3907(5)	−1077(8)	80(6)
O(31)	5435(7)	2816(3)	2500	26(4)	C(19)	8360(12)	5548(4)	2500	32(5)
O(32)	6513(5)	2504(2)	1895(3)	32(3)	C(20)	8615(9)	5393(3)	1960(6)	40(4)
O(33)	2346(6)	2355(3)	1339(4)	56(5)	C(21)	2554(12)	598(5)	2500	50(6)
O(34)	3841(6)	2609(2)	1239(3)	36(4)	C(22)	8684(13)	5865(4)	2500	47(6)
O(35)	2731(6)	2933(2)	1871(4)	43(4)					

[a] Equivalent isotropic *U* defined as one-third of the trace of the orthogonalized $\mathbf{U}_{ij}$ tensor.

shape(s) and size(s) may be selected for efficient crystal packing during the crystallization process.

In a typical hydrothermal procedure, a mixture of $NaMoO_4\cdot 2H_2O$, MoO_3, Mo (−325 mesh), pentaerythritol, Me_3NHCl, Et_4NCl, and H_2O was heated for 3 days at 160 °C. After ramped cooling, dark red-brown crystals of the supercluster $(Me_3NH)_2(Et_4N)Na_4[Na(H_2O)_3H_{15}Mo_{42}O_{109}\{(OCH_2)_3CH_2OH\}_7]\cdot 15H_2O$ (**3**·$15H_2O$) were collected. Upon standing for 10 days, the filtrate deposited red-orange cubic crystals of $(NH_4)_7[NaMo_{16}(OH)_{12}O_{40}]\cdot 4H_2O$ (**1**·$4H_2O$) in *ca.* 20% yield. In an attempt to prepare **1** by a more rational route, the organic cations and pentaerythritol were excluded from the reaction. In

a representative synthesis, a mixture of $Na_2MoO_4 \cdot 2H_2O$, MoO_3, Mo metal, NH_4Cl, and H_2O in the mole ratio 6:6:4:20:300 was heated at 160 °C for 10 h to give **1**·$4H_2O$ in 65% yield.

The infrared spectrum of **1**·$4H_2O$ exhibits a strong band at 946 cm^{-1} attributed to ν(Mo═O) and features at 557 and 535 cm^{-1} assigned to ν(Mo−O−Mo). The absence of prominent features in the 1000−1200 cm^{-1} region, which are characteristic of the presence of the pentaerythritol ligand, confirms that the ligand has not been incorporated into the structure.

Thermal gravimetric analysis of **1**·$4H_2O$ exhibited a 3% weight loss at 110−120 °C, consistent with the loss of 4 water molecules of crystallization. Magnetic susceptibility measurements at room temperature yielded a μ_{eff} of 1.2 μ_B, or 0.35 μ_B per Mo(V) center. The moment appears to arise as a consequence of incomplete spin−spin coupling of the metal−metal-bonded binuclear units.

The analogous potassium-containing compound $(Me_3NH)_4K_2[H_2Mo_{16}(OH)_{12}O_{40}] \cdot 8H_2O$ (**2**·$8H_2O$) was also prepared hydrothermally from the reaction of a mixture of $K_2MoO_4 \cdot 2H_2O$, MoO_3, Mo (−325 mesh), pentaerythritol, Me_3NHCl, Et_4NCl, and H_2O. Curiously, attempts to isolate **2** in the absence of pentaerythritol were unsuccessful.

The infrared spectrum of **2**·$8H_2O$ is similar to that of **1**·$4H_2O$. Likewise, **2**·$8H_2O$ exhibits a low room-temperature moment of 1.25 μ_B (0.36 μ_B per Mo(V) site). The similar magnetic properties of **1**·$4H_2O$, **2**·$8H_2O$ and $(Me_2NH_2)_6[H_2Mo_{16}(OH)_{12}O_{40}]$[25] are consistent with incomplete spin−spin coupling of the Mo(V)−Mo(V) sites rather than of paramagnetic impurities.

As demonstrated in the structural discussion, the K^+ sites of **2**·$8H_2O$ are so disposed as to bridge two neighboring $[H_2Mo_{16}(OH)_{12}O_{40}]^{6-}$ cluster anions (Figure 3) to produce a layer structure of cation-bridged clusters. The cavities within the layers are occupied by Me_3NH^+ cations and H_2O molecules of crystallization. The stacking of layers produces channels enclosing the organic cations and water.

The structure of **2**·$8H_2O$ is reminiscent of heteropolyoxometalates, such as $H_3PW_{12}O_{40} \cdot nH_2O$,[40] which have been shown to be capable of absorbing polar molecules into their bulk structures while retaining their properties as solids.[41] However, the packing in $H_3PW_{12}O_{40} \cdot nH_2O$ precludes entry of nonpolar gaseous molecules into regions between cations and anions, rendering the material nonporous as judged by sorption isotherms.[42] In contrast, salts of heteropolyoxometalates with monovalent cations, such as $M_3PW_{12}O_{40} \cdot nH_2O$ (M = NH_4^+, K^+, or Cs^+) exhibit classical type I sorption isotherms, consistent with the existence of explicitly microporous structures.[41]

In view of the structural similarity of the arrangement of anions and cations in **2**·$8H_2O$ to that observed for the heteropolyanions of the class $M_3PW_{12}O_{40} \cdot nH_2O$, the accessibility of the implicit micropore structure was investigated. Thermal gravimetric analysis of **2**·$8H_2O$ showed a 5% weight loss between 100 and 130 °C corresponding to the loss of the water of crystallization. Powder diffraction studies indicated that the structural integrity of the ionic framework had been maintained. Decomposition of the organo amine occurred in the temperature range 250−400 °C, resulting in a weight loss of *ca*. 10% (10.4% calculated for trimethylamine) and concomitant oxidation of the anion, as indicated by a color change from orange-red to light yellow. To test the microporosity of the material, isotherms

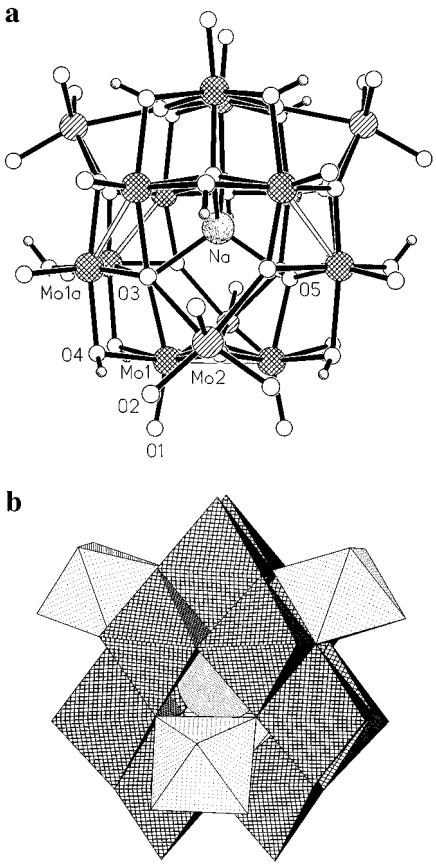

Figure 1. (a) View of the structure of the molecular anion $[NaMo_{16}(OH)_{12}O_{40}]^{7-}$ of **1**·$4H_2O$. (b) Polyhedral representation of the cluster structure viewed along the crystallographic 3-fold axis. The Mo(V) sites of the $\{H_{12}Mo_{12}O_{40}\}^{8-}$ core are represented by cross-hatched octahedra, while the Mo(VI) caps are shown as dotted octahedra. The trioxomolybdenum(VI) units occupy positions on the hexagonal faces of the $\{H_{12}M_{12}O_{40}\}^{8-}$ core. The location of the encapsulated Na^+ cation is illustrated as a highlighted sphere.

with water as adsorbate were investigated. Finely powdered samples of **2**·$8H_2O$ were degassed 24 h at temperatures between 100 and 200 °C in vacuum. As these samples did not absorb water in any significant amount, we conclude that the material is not microporous.

In this regard, it should be noted that the classification of materials as microporous has become considerably obscured by recent claims of microporosity which are either unsupported by experimental results or demonstrably false.[43,44] The test of microporosity for a material is that it exhibits a type I sorption isotherm.[42] The mere existence of channels or incipient voids in the crystal structure of material[43,44] does **not** *ipso facto* constitute demonstration of microporosity. In fact, many complex anion/cation structures when properly oriented display such tunnel or cage structures, and certainly the vast majority do not conform to the classical definition of microporosity. Certainly, a material such as $(H_3N(CH_2)_6NH_3)_6[W_{18}P_2O_{62}] \cdot 3H_2O$,[44] which demonstrably fails to sorb either H_2O or N_2 in significant amounts, cannot be termed microporous.

(b) The "Superclusters": $(Me_3NH)_2(Et_4N)Na_4[Na(H_2O)_3H_{15}Mo_{42}O_{109}\{(OCH_2)_3CCH_2OH\}_7] \cdot 15H_2O$ (3·$15H_2O$), $(Me_3NH)_2(H_3O)Na_6[Na(H_2O)_3H_{13}Mo_{42}O_{109}\{(OCH_2)_3CCH_2OH\}_7] \cdot 7H_2O$ (4·$7H_2O$), $Na_9[(MoO_3)H_{14}Mo_{42}O_{109}\{(OCH_2)_3CCH_2OH\}_7] \cdot 0.5C(CH_2OH)_4 \cdot 25H_2O$ (5·$0.5C(CH_2OH)_4 \cdot 25H_2O$),

(40) Brown, C. M.; Noe-Spirlet, M. R.; Busing, W. R.; Levy, H. A. *Acta Crystallogr.* **1977**, *B33*, 1038.
(41) Moffat, J. B. *J. Mol. Catal.* **1989**, *52*, 169.
(42) Ruthven, D. M. *Principles of Absorption and Adsorption Processes;* John Wiley & Sons: New York, 1984.
(43) Farrell, R. P.; Hambley, T. W.; Lay, P. A. *Inorg. Chem.* **1995**, *34*, 757.
(44) Hölscher, M.; Englert, U.; Zibrowius, B.; Hölderich, W. *Angew. Chem., Int. Ed. Engl.* **1994**, *33*, 2491.

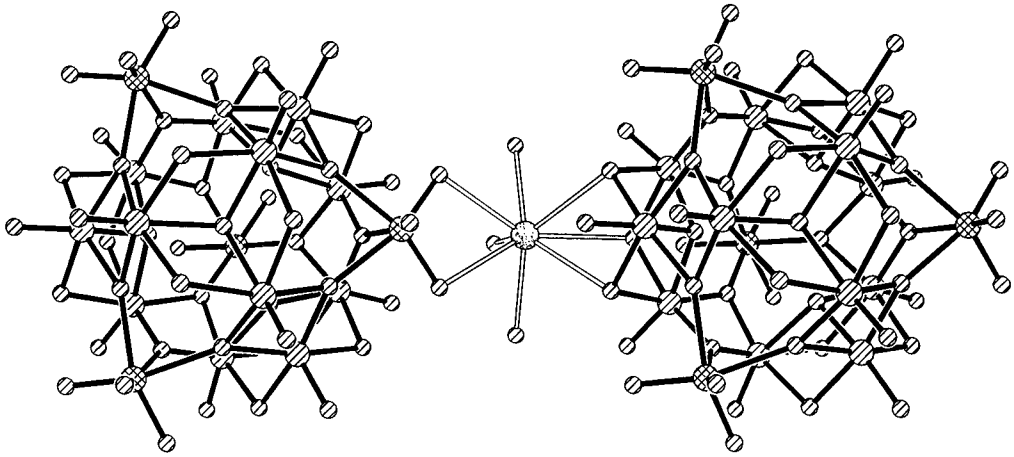

Figure 2. Ball and stick representation of the linking of a two adjacent $[H_2Mo_{16}(OH)_{12}O_{40}]^{6-}$ (**2a**) clusters through a $[K(H_2O)_3]^+$ unit.

and $(Mo_4N)(Et_2NH_2)(H_3O)_2Na_6[(MoO_3)H_{13}Mo_{42}O_{109}\{(OCH_2)_3CCH_3\}_7]\cdot 10H_2O$ ($6\cdot 10H_2O$). The materials of the Mo−O−alkoxide class, **3**−**6**, can be synthesized by analogous hydrothermal methods. In the representative synthesis described previously, dark red-brown crystals of $\mathbf{3}\cdot 15H_2O$ were produced in *ca*. 55% yield. The infrared spectrum exhibited bands of strong intensity at 886, 911, and 968 cm^{-1} associated with ν(Mo═O) for the different oxomolybdenum environments. The features at 911 and 886 cm^{-1} may be attributed to the symmetric and asymmetric stretching modes of the *cis*-dioxomolybdate $\{Mo^{VI}O_2\}$ units, while the 968 cm^{-1} band is reasonable for the Mo(V) sites with a single terminal oxo group. The bands at 1112, 1061, and 1021 cm^{-1} are in the characteristic region for ligand bands, with the latter assigned to ν(C−O).

Compound $\mathbf{4}\cdot 7H_2O$ is prepared in a similar fashion, by omitting Et_4NCl and Mo metal from the starting mixture and modifying the reactantsratios. The infrared spectrum is similar to that of $\mathbf{3}\cdot 15H_2O$ with ν(Mo═O) bands at 890, 918 and 975 cm^{-1} and characteristic ligand bands at 1015 and 1110 cm^{-1}.

While **3** and **4** contain the $\{Na(H_2O)_3\}^+$ unit in the anion cluster cavity (*vide infra*), minor modifications in reaction conditions produce the $\{MoO_3\}$ encapsulated species $\mathbf{5}\cdot 25H_2O\cdot 0.5C(CH_2OH)_4$ and $\mathbf{6}\cdot 10H_2O$. In the case of $\mathbf{6}\cdot 10H_2O$, the tris(hydroxymethyl)ethane ligand derivative is used in place of pentaerythritol, while **5** is prepared in the absence of organoammonium cations. The infrared spectra of **5** and **6** are similar to those of **3** and **4**, with ν(Mo═O) bands in the 885−970 cm^{-1} region and ligand bands in the 1010−1130 cm^{-1} range.

Since the $\{Mo_{16}O_{52}\}$ unit common to **1** and **2** provides the structural core of the superclusters **5** and **6** as described in the following section, the synthesis of the superclusters from $[H_{14}Mo_{16}O_{52}]^{6-}$ was investigated. In this fashion, the hydrothermal reaction of a solution of $\mathbf{2}\cdot 8H_2O$ with Me_3NHCl, $Na_2MoO_4\cdot 2H_2O$, and pentaerythritol was found to give **4** in *ca*. 80% yield. An analogous reaction, employing $Na_2MoO_4\cdot 2H_2O$, MoO_3, Me_4NCl, Et_2NH, and tris(hydroxymethyl)ethane yielded **6** in *ca*. 65% yield.

Although these fragment condensation processes, shown in the following schematic diagram, provide a satisfactory conceptual framework for the preparation of tailor-made clusters by control of inorganic hydrolysis−condensation and aggregation reactions, structural organization of the constituent subunits relies on self-assembly. However, while mechanistic details for the assembly of such aggregates are sketchy at best, the reactive, highly negatively charged and nucleophilic $\{H_{12}Mo_{16}O_{52}\}^{8-}$ unit may provide a structural core for linkage of appropriate subunits to produce the supercluster. It has been noted that reduction of polyoxometalate clusters increases the basicity of the surface oxo groups, predominantly the bridging oxygens, and concomitantly the reactivity of the species with electrophilic groups. One example is provided by the reduction of $[PMo_{12}O_{40}]^{3-}$ to $[PMo_{12}O_{40}]^{4-}$, which subsequently reacts with $[MoO_3]$ to give $[PMo_{14}O_{44}]^{4-}$, an α-Keggin core with two $\{MoO_2\}$ units fused onto opposite tetragonal faces of the Keggin core.[45]

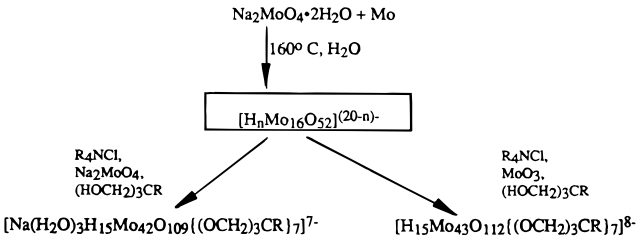

Description of the Structures. (a) The Hexadecamolybdenum Oxide Clusters: $(NH_4)_7[NaMo_{16}(OH)_{12}O_{40}]\cdot 4H_2O$ ($\mathbf{1}\cdot 4H_2O$) and $(Me_3NH)_4K_2[H_2Mo_{16}(OH)_{12}O_{40}]\cdot 8H_2O$ ($\mathbf{2}\cdot 8H_2O$). As shown in Figure 1, X-ray structural analysis of $\mathbf{1}\cdot 4H_2O$ revealed the presence of discrete, ordered $[Mo_{16}(OH)_{12}O_{40}]^{8-}$ anions, with a central cavity encapsulating a Na^+ cation. The anion contains 4 Mo(VI) sites, 12 Mo(V) centers, 40 terminal and bridging oxo groups, and 12 bridging hydroxy groups in full tetrahedral symmetry. The 12 Mo(V) centers of **1** form six metal−metal-bonded binuclear units with a Mo···Mo distance of 2.62(1) Å. The four *facial* $\{Mo^{VI}O_3\}$ "anti-Lipscomb" units[46] cap four of the eight $\{Mo_3O_3\}$ faces of the Mo^{V}_{12} truncated tetrahedron with the four Mo(VI) sites forming an expanded Mo_4 tetrahedron. Such *fac* $\{MoO_3\}$ units are predicted to be unstable in polyanion frameworks as a consequence of the strong *trans* influence of the M−O(terminal) groups which would result in weak bonding to the opposite $\{MO_3\}$ face of the $\{MO_6\}$ octahedron and consequent dissociation. While the *fac* $\{MoO_3\}$ unit has been observed, examples are limited to simple coordination complexes such as $[MoO_3(dien)]$,[47] $[(MoO_3)_2(EDTA)]^{4-}$,[48] and $[MoO_3\{N(CH_2CO_2)_3\}]^{3-}$ [49] or to polyoxomolybdate species derivatized by coordination of

(45) Khan, M. I.; Chen, Q.; Zubieta, J. Unpublished results.
(46) Lipscomb, W. N. *Inorg. Chem.* **1965**, *4*, 132.
(47) Cotton, F. A.; Elder, R. C. *Inorg. Chem.* **1964**, *3*, 397.
(48) Parks, J. J.; Glick, M. D.; Hoard, J. L. *J. Am. Chem. Soc.* **1969**, *91*, 301.
(49) Butcher, R. J.; Penfold, B. R. *J. Cryst. Mol. Struct.* **1976**, *6*, 13.

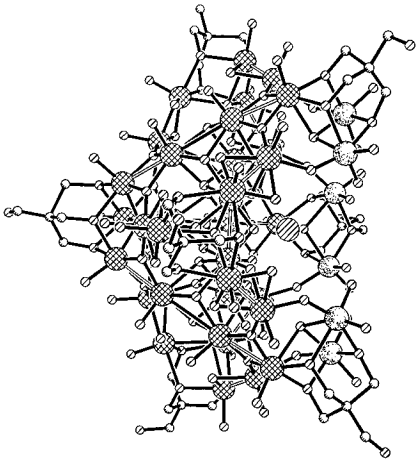

Figure 3. View of the structure of the anionic cluster $[Na(H_2O)_3H_{15}Mo_{42}O_{109}\{(OCH_2)_3CCH_2OH\}_7]^{7-}$ (**3a**) of **3**·15H_2O. The Mo(V) sites are represented as cross-hatched spheres, while the Mo(VI) centers are shown as lightly highlighted spheres. The Na^+ cation, illustrated as a sphere lined bottom left to top right, occupies the molecular cavity of **3a**, whose "lid" is provided by the six $\{Mo^{VI}O_2\}^{2+}$ units of the cluster.

organic ligands, as represented by $[Mo_3O_7\{(OCH_2)_3CCH_3\}_2]^{2-}$.[35,50]

As shown in the polyhedral representation of Figure 1b, the four Mo(VI) atoms cap hexagonal faces of the central $\{Mo_{12}O_{40}\}$ core. Reduction of the molybdenum sites of the central core to the Mo(V) oxidation state significantly increases the basicity of the surface oxygens, allowing aggregation of the electrophilic $\{MoO_3\}$ units. The 12 oxygen atoms of the molecular anion are of five distinct types. The 12 O(1) oxygens are each terminally bonded to a Mo(V) atom of the $\{Mo_{12}O_{40}\}$ core at a distance of 1.69(2) Å. The 12 O(2) oxygens are associated with the four *facial* trioxomolybdate $\{Mo^{VI}O_3\}$ capping units as strongly bonded terminal oxo groups with a Mo(2)−O(2) distance of 1.74(3) Å. Each of the 12 O(3) oxygen atoms adopts a μ_3 bonding mode between two Mo(V) centers from adjacent binuclear units and one Mo(2) site; the bridging to the Mo(1) sites is unsymmetrical with Mo(1)−O(3) distances of 1.89(3) and 2.08(3) Å, while the Mo(2)−O(3) distance is 2.22(3) Å. The Mo(1)−O(4) bond distances of 2.14(4) and 2.09(3) Å and valence sum calculations[51] identify the 12 O(4) sites as doubly bridging hydroxy groups. Although the proton locations could not be unambiguously assigned from the X-ray analysis, the most likely site locates the protons so as to form intramolecular hydrogen-bonding interactions with the O(2) centers, with O(2)···O(4) and O(2)···H(4) distances of 2.82 and 1.89 Å, respectively. The four O(5) oxygen atoms define the perimeter of the cavity formed by the molybdenum−oxygen cage, and each adopts a μ_4 bridging mode with regard to three Mo(V) sites, each from an adjacent pair of binuclear units, and to the encapsulated and tetrahedrally coordinated Na^+ cation. The Mo(1)−O(5) and Na−O(5) distances are 2.10(1) and 2.18(3) Å, respectively. While the Na−O distances are relatively short, they are consistent with those previously reported for Na^+ cations held between hexanuclear molybdophosphate units in materials such as $[(H_3O)_2NaMo_6P_4O_{24}(OH)_7]^{2-}$ [52] and $[Na\{H_3Mo_6O_{15}(O_3PC_6H_5)_4\}_2]^{15-}$.[53−55] Although the low coordination number for Na^+ is likewise unusual, it is not without precedent,[56] and a similar tetrahedral environment has been described for the encapsulated Na^+ cation of $[Na(i\text{-}PrSn)_{12}O_4(OH)_{24}]^{5+}$,[57] suggesting that the geometric requirements of the metal−oxo cage dictate the environment of the cavity.

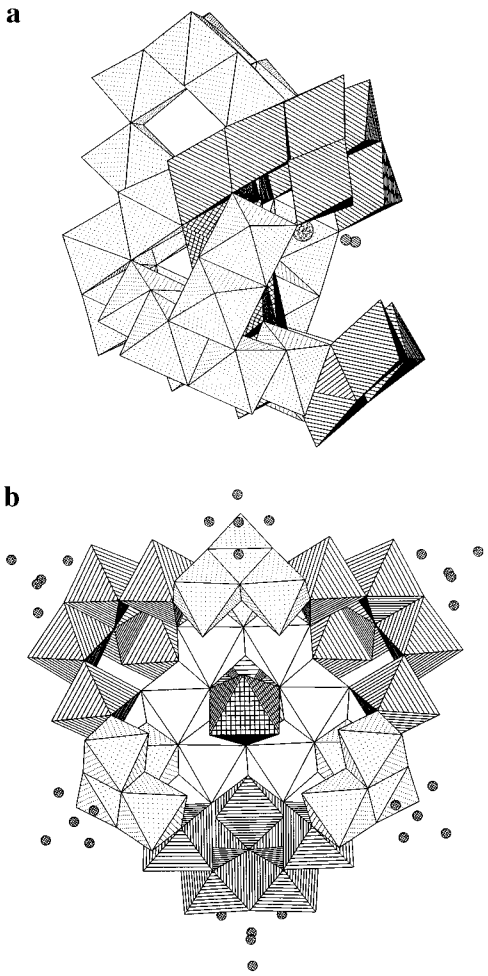

Figure 4. (a) Polyhedral representation of the structure of **3a**, adopting the orientation of Figure 3 and illustrating the projection of the $\{Mo^{VI}O_2\}$ groups of subunits **3B** from the central core of the anionic cluster and the position of the $\{Na(H_2O)_3\}^+$ grouping in the cavity thus formed. The lined octahedra represent the Mo sites of subunit **3B**, while the dotted octahedra illustrate **3A** and **3A′** types and the cross-hatched octahedra the Mo sites of the central hexanuclear ring (*vide infra*). The Na^+ and H_2O positions are represented by spheres. (b) Polyhedral representation of **3a** viewed along the approximate 3-fold axis of the cluster. The Mo centers of the central ring are clear octahedra, the **3A** and **3A′** sites are dotted octahedra, and the **3B** sites are lined. The central cross-hatched octahedron represents the $Na(H_2O)_3^+$ groupings of **3** and **4** or the $\{MoO_3\}$ units of **5** and **6**.

Since the central cavity of the anionic cluster of **1** exhibits dimensions barely adequate to accommodate a Na^+ cation, the consequences of replacing Na^+ with larger cations were investigated. In this fashion, introduction of the K^+ cation, whose ionic radius precludes encapsulation in the small cavity of the cluster, resulted in isolation of **2**·8H_2O, a species exhibiting a $\{Mo_{16}O_{52}\}$ core essentially identical to that of **1**·4H_2O. In this instance, however, the central cavity is occupied by two protons.

The four oxygen atoms which define the cavity perimeter for **1** exhibit valence sums of 1.19−1.35, suggesting that these sites are partially protonated. In view of the charge requirements

(50) Hider, R. N.; Wilkins, C. J. *J. Chem. Soc., Dalton Trans.* **1984**, 495.
(51) Brown, I. D. In *Structure and Bonding in Crystals*; O'Keefe, M., Navrotsky, A., Eds.: Academic Press: New York, 1981; Vol. II, p 1.
(52) Haushalter, R. C.; Lei, F. W. *Inorg. Chem.* **1989**, *28*, 2905.
(53) Cao, G.; Haushalter, R. C.; Strohmaier, K. G. *Inorg. Chem.* **1993**, *32*, 127.
(54) Khan, M. I.; Chen, Q.; Zubieta, J. *Inorg. Chim. Acta* **1993**, *206*, 131.
(55) Khan, M. I.; Chen, Q.; Zubieta, J. *Inorg. Chim. Acta* **1995**, *231*, 13.
(56) Shannon, R. D. *Acta Crystallogr., Sect. A* **1976**, *32*, 751.
(57) Reuter, H. *Angew. Chem., Int. Ed. Engl.* **1991**, *30*, 1482.

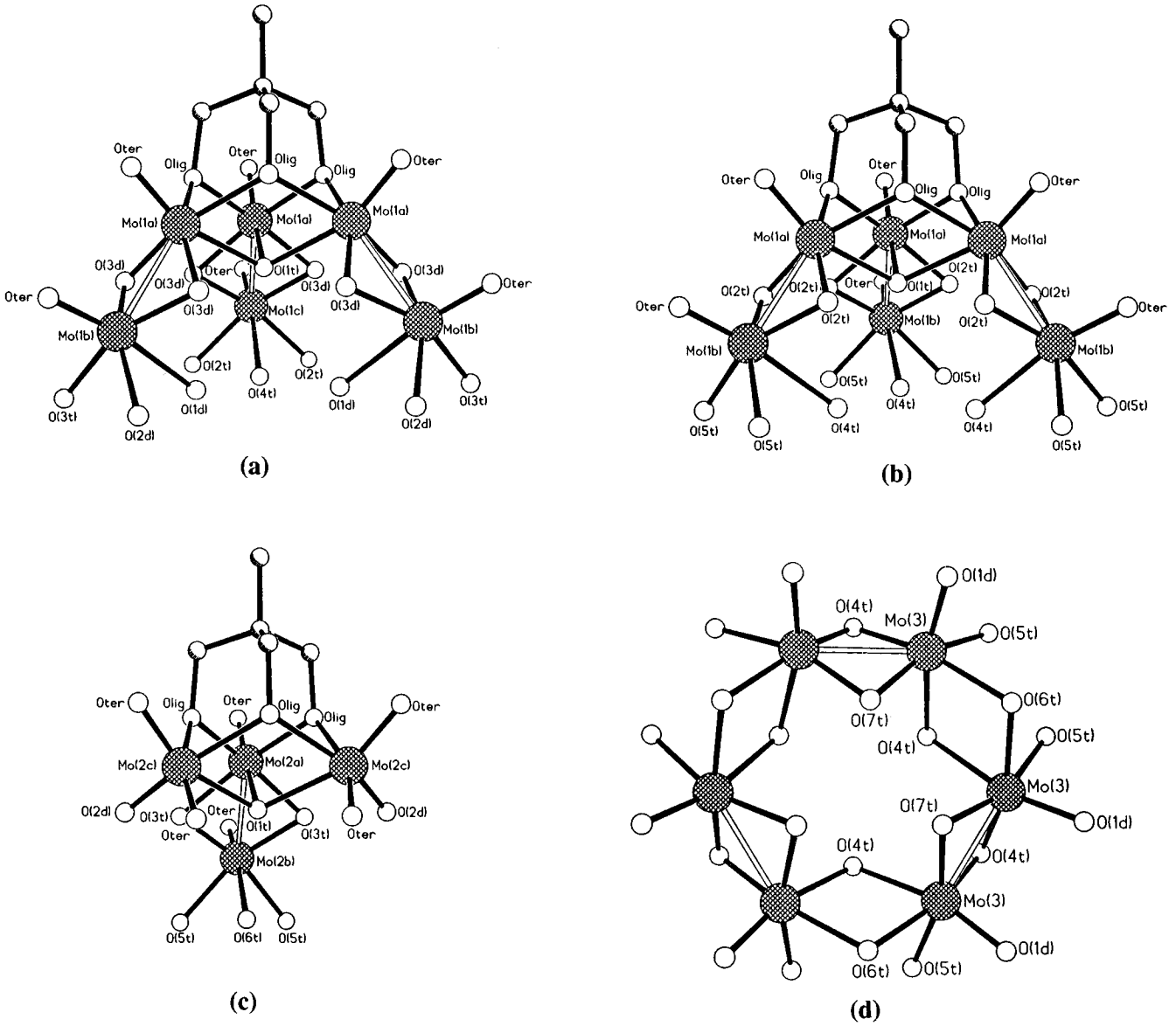

Figure 5. The four building blocks of the cluster cores of **3**−**6**: (a) the hexanuclear Mo(V)−ligand subunit $\{Mo^{V}_{6}O_{22}[(OCH_2)_3CR]\}$ (**3A**) of which there are three in the molecular anion cluster; (b) the hexanuclear unit $\{Mo^{V}_{6}O_{22}[(OCH_2)_3CR]\}$ (**3A′**), which adopts the unique central position in the clusters, providing the linchpin for the construction of the clusters; (c) the tetranuclear mixed-valence site $\{Mo^{V}_{2}Mo^{VI}_{2}O_{15}[(OCH_2)_3CR]\}$ (**3B**), which contributes three subunits to the cluster framework; (d) the unique central hexanuclear Mo(V) ring $\{Mo_6O_{24}\}$ (**3C**). The oxygen atom labeling scheme adopted for the anion clusters of **3**−**6** is also shown: O_{ter}, terminal oxo groups; O_{lig}, ligand alkoxy oxygen donors; O(1d), bridge Mo(1b) site of subunit **3A** to Mo(3) of the central ring **3C**; O(2d), bridge Mo(1b) sites of **3A** to Mo(2c) centers of **3B**; O(3d), link Mo(1a) and Mo(1b) sites within a **3A** subunit; O(1t), bridge triangular arrays of alkoxide oxygen linked Mo(1a), Mo(2a), or Mo(2c) sites of subunits **3A**, **3A′**, or **3B**, respectively; O(2t), bridge Mo(1a)′ and Mo(1b)′ sites of a **3A′** subunit to an Mo(1c) site of **3A**; O(3t), bridge Mo(2a) and Mo(2b) sites of **3B** to Mo(1b) of **3A**; O(4t), bridge Mo(1c) of **3A** or Mo(1b)′ of **3A′** to two Mo(3) centers of **3C**; O(5t), link an Mo(1b)′ site of **3A′** to Mo(2b) of **3B** and Mo(3) of **3C**; O(6t), bridge two adjacent Mo(3) sites of **3C** to an Mo(2b) of **3B**; O(7t), link two adjacent Mo(3) sites of **3C** to the guest group, $Na(H_2O)_3^+$ in **3** and **4** or $\{MoO_3\}$ in **5** and **6**.

of the $[Mo_{16}(OH)_{12}O_{40}]^{8-}$ host and the obvious cation occupancy of the $[NaMo_{16}(OH)_{12}O_{40}]^{7-}$ core of **1**, the cavity of **2** appears to be occupied by 2 H^+, a situation reminiscent of the internal protons encountered for $[H_2W_{12}O_{40}]^{6-}$.[58] While this cavity may accommodate four protons, as suggested for **5** and **6**, double occupancy is consistent with the molybdenum mean oxidation state for **2** as determined by valence-bond calculations.[51]

The central $\{Mo_{12}O_{40}\}$ core of the molecular anions of **1** and **2** adopts a metal−oxygen framework classified as the ϵ-Keggin type[59] and previously observed for the clusters $[Al_{13}O_4(OH)_{24}(H_2O)_{12}]^{7+}$,[60] $[Al_{13}O_4(OH)_{25}(H_2O)_{11}]^{6+}$,[61] $[H_3Mn_3V_{12}O_{40}]^{5-}$,[62] and $[(C_5Me_5Rh)_8(Mo^{V}_{12}O_{36})(Mo^{VI}O_4)]^{2+}$.[63] It is instructive to compare the structure of the central $\{Mo_{13}O_{40}\}$ core of this latter cationic cluster to the $\{H_2Mo_{12}O_{40}\}$ and $\{NaMo_{12}O_{40}\}$ cores

(58) Pope, M. T.; Varga, G. M., Jr. *J. Chem. Soc., Chem. Commun.* **1966**, 653.
(59) Baker, L. C. W.; Figgis, J. S. *J. Am. Chem. Soc.* **1970**, *92*, 3794.
(60) Johansson, G. *Ark. Kemi* **1963**, *20*, 305.
(61) Johansson, G. Ark. *Kemi* **1963**, *20*, 321.
(62) Ichida, H.; Nagai, K.; Sasaki, Y.; Pope, M. T. *J. Am. Chem. Soc.* **1989**, *111*, 586.
(63) Chae, H. K.; Klemperer, W. G.; Paiz Loyo, D. E.; Day, V. W.; Eberspacher, T. A. *Inorg. Chem.* **1992**, *31*, 3187.
(64) Stiefel, E. I. *Prog. Inorg. Chem.* **1977**, *22*, 1.
(65) Sykes, A. G. In *Comprehensive Coordination Chemistry*; Wilkinson, G., Gillard, R. D., McCleverty, J. A., Eds.: Pergamon Press, Oxford, England, 1987; Vol. 3, p 1229.
(66) Khan, M. I.; Zubieta, J. *Prog. Inorg. Chem.*, in press.
(67) Haushalter, R. C.; Mundi, L. A. *Chem. Mater.* **1992**, *4*, 31.
(68) Stein, A.; Keller, S. W.; Mallouk, T. E. *Science* **1993**, *259*, 1558.

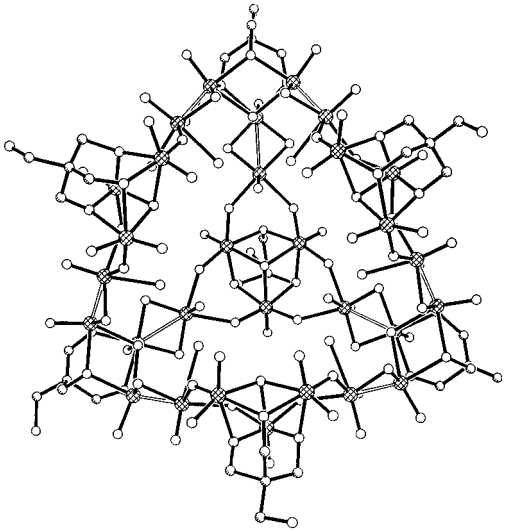

Figure 6. View of the cavity formed by the linking of subunits of types **3A**, **3A′**, and **3B**. The central position of the ring is occupied by the **3A′** subunit.

of **1** and **2**, respectively. In all three cases, the ϵ-Keggin structure allows the octahedral Mo(V) centers to form binuclear units with short Mo···Mo distances and localized Mo···Mo bonds, a characteristic feature of Mo(V) chemistry encountered for isolated binuclear species, reduced polyanions, and even solid phases.[64−67] While the cavity of $[(C_5H_5Rh)_8(Mo^{V}_{12}O_{36})(Mo^{VI}O_4)]^{2+}$ is occupied by a tetrahedrally coordinated Mo(VI) center with short Mo−O distances of 1.75(1) Å, the Na^+ cation of **1** exhibits Na−O distances of 2.18(3) Å, with the cavity diameter defined by O(5)···O(5) distances of 3.3 Å, a value identical to that for the void in **2**·8H_2O. The remarkable flexibility of the host ϵ-$\{Mo^{V}_{12}O_{40}\}$ cage is demonstrated by the isolation of clusters encapsulating cationic guests with such diverse coordination requirements as protons and Na^+. While it is tempting to speculate on the role of the Na^+ cation in **1** as a template for the construction of the host framework, the details of templating mechanisms remain obscure. A given template can produce different structures, while the same structure may be isolated from different templates, as may be the case for **1** and **2** with Na^+ cations and protons serving as the templates. Evidently, charge-compensating and space-filling requirements play a significant role in the isolation of **1** and **2**.[68]

While the K^+ cations of **2** cannot be accommodated in the anion cavities, they do serve an important structural role in bridging neighboring clusters to form a 2-D network, as illustrated in Figure 2. Each cluster is linked to each of four adjacent clusters in the sheet through a $K(H_2O)_3^+$ unit. The network of anion clusters and cations produces cavities within the layers which are occupied by H_2O molecules. The region between these inorganic layers is occupied by the $(Me_3NH)^+$ cations to produce a repeating motif of alternating inorganic and organic layers. Since structures of this type characteristically segregate into hydrophobic and hydrophilic domains,[67] this arrangement is common and provides no necessary implication of microporosity for the material.

It is also noteworthy that **1** and **2** are isolated from similar reaction mixtures as those used to produce the superclusters **3**−**6**. As discussed below, the $\{Mo_{16}O_{52}\}$ cage serves as the core of the anionic clusters **5** and **6** and suggests that preassembly of such structural units in solution may be involved in the cluster aggregation process.

(b) The "Superclusters": $(Me_3NH)_2(Et_4N)Na_4[Na(H_2O)_3H_{15}Mo_{42}O_{109}\{(OCH_2)_3CCH_2OH\}_7]\cdot 15H_2O$ (3·15H_2O), $(Me_3NH)_2(H_3O)Na_6[Na(H_2O)_3H_{13}Mo_{42}O_{109}\{(OCH_2)_3CCH_2OH\}_7]\cdot 7H_2O$ (4·7H_2O), $Na_9[(MoO_3)H_{14}Mo_{42}O_{109}\{(OCH_2)_3CCH_2OH\}_7]\cdot 25H_2O\cdot 0.5C(CH_2OH)_4$ (5·25H_2O·0.5C$(CH_2OH)_4$), and $(Me_4N)(Et_2NH_2)(H_3O)_2Na_6[(MoO_3)H_{13}Mo_{42}O_{109}\{(OCH_2)_3CCH_3\}_7]\cdot 10H_2O$ (6·10H_2O). The X-ray structures of **3**−**6** revealed that all share a common discrete, molecular anionic aggregate $[H_nMo_{42}O_{109}\{(OCH_2)_3CR\}_7]^{(23-n)-}$, which is shown in Figure 3 for the cluster incorporating the $Na(H_2O)_3^+$ unit, namely $[Na(H_2O)_3H_{15}Mo_{42}O_{109}\{(OCH_2)_3CCH_2OH\}_7]^{7-}$ (**3a**). As illustrated in the polyhedral representation of Figure 4, the structure consists of a framework of edge- and corner-sharing $\{MoO_6\}$ octahedra with the organic residues projecting outward from the central core. The structure of anion may be constructed from the fundamental building blocks illustrated in Figure 5. There are four units of type **3A**, which consist of the trishydroxymethylalkane ligands, $[RC(CH_2O)_3]^{3-}$,

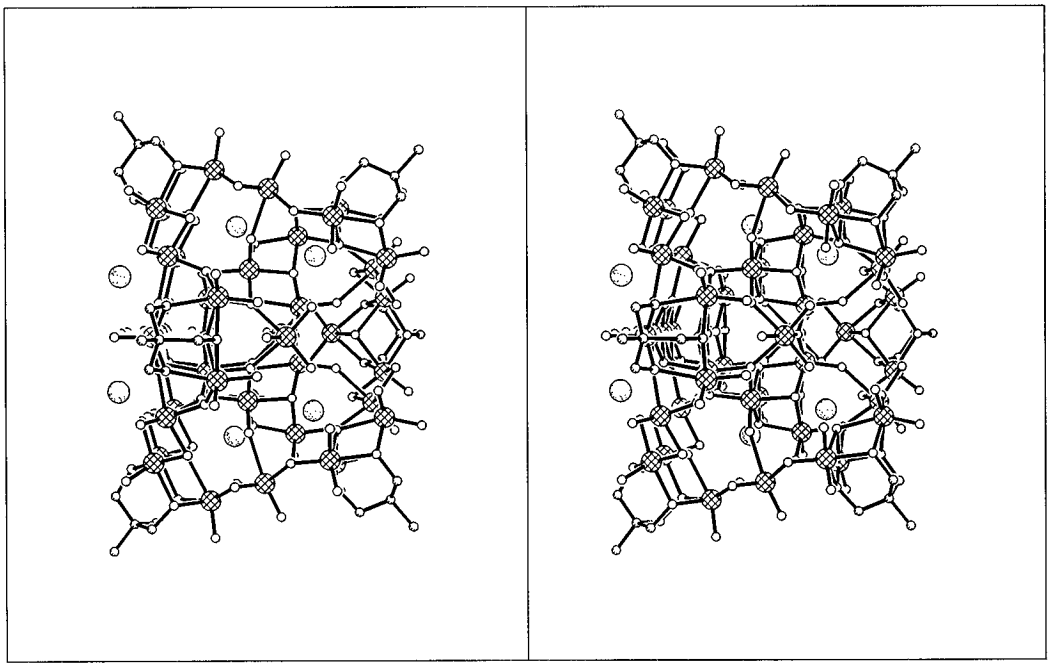

Figure 7. Stereoview of the structure of the $[(MoO_3)H_{13}Mo_{42}O_{109}\{(OCH_2)_3CCH_3\}_7]^{10-}$ anion cluster of **6** and of the six associated Na^+ cations.

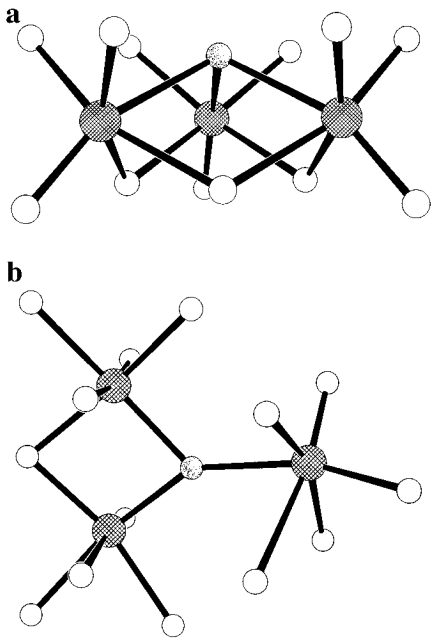

Figure 8. (a) View of a typical pyramidal triply-bridging oxo site, which is illustrated by heavy shading. These sites either bond to the Na^+ centers associated with the cluster or are protonated. (b) The "Y"-shaped planar sites adopted by the remaining triply-bridging oxo groups. Valence-bond calculations and geometry preclude these sites from protonation.

Table 10. Oxygen Atom Types for the $\{XMo_{42}O_{130}\}$ Cores of **3**−**6** ($X = Na(H_2O)_3^+$ for **3** and **4**; $X = MoO_3$ for **5** and **6**)

designator	subunits bridged or location description	total no. of oxygens of this type
O_{ter}	terminal {MoO} groups on Mo(1a), Mo(1b), Mo(1a)′, Mo(1b)′, Mo(2a), Mo(2b)	30
	terminal $\{MoO_2\}$ groups on Mo(2c)	12
O_{lig}	ligand alkoxy oxygens	21
O(1d)	**3A**/**3C** (Mo(1b)−Mo(3))	6
O(2d)	**3A**/**3B** (Mo(1b)−Mo(2c))	6
O(3d)	**3A** (Mo(1a)−Mo(1b))	18
O(1t)	**3A**, **3A′**, **3B** (3×Mo(1a), 3×Mo(1a)′, Mo(2a)−2×Mo(2c))	7
O(2t)	**3A**/**3A′** (Mo(1c)−Mo(1a)′−Mo(1b)′)	6
O(3t)	**3A**/**3B** (Mo(1b)−Mo(2a)−Mo(2b))	6
O(4t)	**3A**/**3C** or **3A′**/**3C** (Mo(1c)−2×Mo(3) and Mo(1b)′−2×Mo(3))	6
O(5t)	**3A′**/**3B**/**3C** (Mo(1b)′−Mo(2b)−Mo(3))	6
O(6t)	**3B**/**3C** (Mo(2b)−2×Mo(3))	3
O(7t)	**3C**/guest (2×Mo(3)−$Na(H_2O)_3^+$, or 2×Mo(3)−MoO_3)	3

coordinated in the characteristic tridentate bridging mode to a triangular arrangement of three Mo(V) centers, each of which is in turn bridged through two *cis* oxo groups to an adjacent Mo(V) site. One of these hexamolybdenum(V) units (**3A′**) is distinguished from the other three by the nature of the oxo groups which link it to its adjacent cluster subunits. By virtue of its central location in the cluster, shown in Figure 6, subunit **3A′** bridges to the three **3A** subunits, as well as to the **3B** and **3C** fragments. Consequently, the doubly bridging oxo groups of the **3A** type subunits assume the triply bridging mode in **3A′**, while the triply bridging oxygen atoms link different subunits.

The second structural unit **3B**, of which there are three present in the anion cluster, consists of the tridentate alkoxide ligand bridging a triangular arrangement of one Mo(V) and two Mo(VI) sites. The Mo(V) site is associated through edge-sharing by two oxo groups with an exocyclic Mo(V) site. The Mo−Mo distances for the Mo(V) binuclear units of **3A**, **3A′**, and **3B** exhibit the characteristic short interaction distance, in the range 2.55−2.65 Å, associated with a Mo(V)−Mo(V) single bond.

Table 11. Selected Bond Lengths (Å) for the Molecular Anions of **3**−**6**

	cluster identities			
	3	**4**	**5**	**6**
		Subunit **3A**		
Mo(1a)−O_{ter}	1.67(2)	1.68(2)	1.67(3)	1.67(2)
Mo(1a)−O_{lig}	2.12(2)	2.13(2)	2.13(2)	2.13(2)
Mo(1a)−O(1t)	2.20(2)	2.24(2)	2.23(2)	2.26(2)
Mo(1a)−O(3d)	1.91(2)	1.93(2)	1.92(2)	1.94(2)
Mo(1b)−O_{ter}	1.66(2)	1.68(2)	1.67(2)	1.67(2)
Mo(1b)−O(1d)	2.40(2)	2.39(2)	2.41(2)	2.40(2)
Mo(1b)−O(2d)	2.04(2)	2.06(2)	2.06(2)	2.05(2)
Mo(1b)−O(3d)	1.93(2)	1.94(2)	1.94(2)	1.94(2)
Mo(1b)−O(3t)	2.10(2)	2.10(2)	2.09(2)	2.11(2)
Mo(1c)−O_{ter}	1.65(2)	1.69(2)	1.67(2)	1.66(2)
Mo(1c)−O(3d)	1.93(2)	1.94(2)	1.93(2)	1.94(2)
Mo(1c)−O(2t)	2.13(2)	2.24(2)	2.12(2)	2.12(2)
Mo(1c)−O(4t)	2.29(2)	2.25(2)	2.26(2)	2.27(2)
		Subunit **3A′**		
Mo(1a)′−O_{ter}	1.67(2)	1.68(2)	1.68(2)	1.69(2)
Mo(1a)′−O_{lig}	2.10(2)	2.11(2)	2.10(2)	2.11(2)
Mo(1a)′−O(1t)	2.09(2)	2.10(2)	2.09(2)	2.09(2)
Mo(1a)′−O(2t)	1.96(2)	1.98(2)	1.97(2)	1.98(2)
Mo(1b)′−Oter	1.68(2)	1.68(2)	1.67(3)	1.68(2)
Mo(1b)′−O(2t)	1.97(2)	1.98(2)	1.98(3)	1.98(2)
Mo(1b)′−O(4t)	2.18(2)	2.17(2)	2.18(3)	2.21(2)
Mo(1b)′−O(5t)	2.06(2)	2.05(2)	2.06(3)	2.08(2)
		Subunit **3B**		
Mo(2a)−O_{ter}	1.67(2)	1.65(2)	1.66(3)	1.67(2)
Mo(2a)−O_{lig}	2.14(2)	2.13(2)	2.14(3)	2.14(2)
Mo(2a)−O(1t)	2.24(2)	2.23(2)	2.24(2)	2.23(2)
Mo(2a)−O(3t)	1.98(2)	1.98(2)	1.99(2)	1.98(2)
Mo(2b)−O_{ter}	1.66(2)	1.67(3)	1.68(3)	1.68(2)
Mo(2b)−O(3t)	1.98(2)	1.97(2)	1.98(2)	1.98(2)
Mo(2b)−O(5t)	2.07(2)	2.07(2)	2.08(2)	2.09(2)
Mo(2b)−O(6t)	2.25(2)	2.26(2)	2.26(2)	2.25(2)
Mo(2c)−O_{ter}	1.70(2)	1.71(2)	1.70(3)	1.71(2)
Mo(2c)−O_{lig}	2.23(2), 2.13(2)	2.22(2), 2.14(2)	2.23(2), 2.13(2)	2.22(2), 2.14(2)
Mo(2c)−O(1t)	2.22(2)	2.21(2)	2.22(2)	2.23(2)
Mo(2c)−O(2d)	1.81(2)	1.80(2)	1.80(2)	1.81(2)
		Subunit **3C**		
Mo(3)−O(1d)	1.71(2)	1.70(2)	1.71(3)	1.72(2)
Mo(3)−O(4t)	2.14(2), 1.96(2)	2.11(2), 1.98(2)	2.12(2), 1.98(2)	2.16(2), 1.98(2)
Mo(3)−O(5t)	2.11(2)	2.12(2)	2.12(2)	2.09(2)
Mo(3)−O(6t)	2.08(2)	2.10(2)	2.09(2)	2.06(2)
Mo(3)−O(7t)	1.92(2)	1.93(2)	1.93(2)	1.93(2)
		Guest		
Na−O(7t)	2.33(2)	2.29(2)		
Na−OH_2	2.55(2)	2.54(2)		
Mo−O(7t)			2.25(2)	2.28(2)
Mo═O			1.77(3)	1.77(3)

The third subunit, **3C**, exhibits a six-membered Mo(V) ring $\{Mo_6O_{24}\}$ of edge-sharing octahedra with alternating short−long Mo(V)−Mo(V) distances. The ring **3C** is linked through its oxo groups to the three **3A**, three **3B**, and the unique **3A′** subunits. The subunit **3A′** caps one face of the ring, while the opposite face is directed toward the molecular cavity of the anion and occupied either by a $Na(H_2O)_3^+$ unit in **3** and **4** or by a $\{MoO_3\}$ unit in **5** and **6**.

The tetranuclear subunits **3B** project outward from the core of the cluster, in the fashion of the arms of a grapple, thus producing a cavity with an atom to atom diameter of *ca.* 7 Å. The perimeter of this cavity is defined by the central ring **3C** and the three **3B** subunits, with six terminal oxo groups, one from each *cis*-dioxo Mo(VI) group of these latter fragments, forming the "pincers" of the grapple arms and constricting the cavity aperture, as shown in Figure 7.

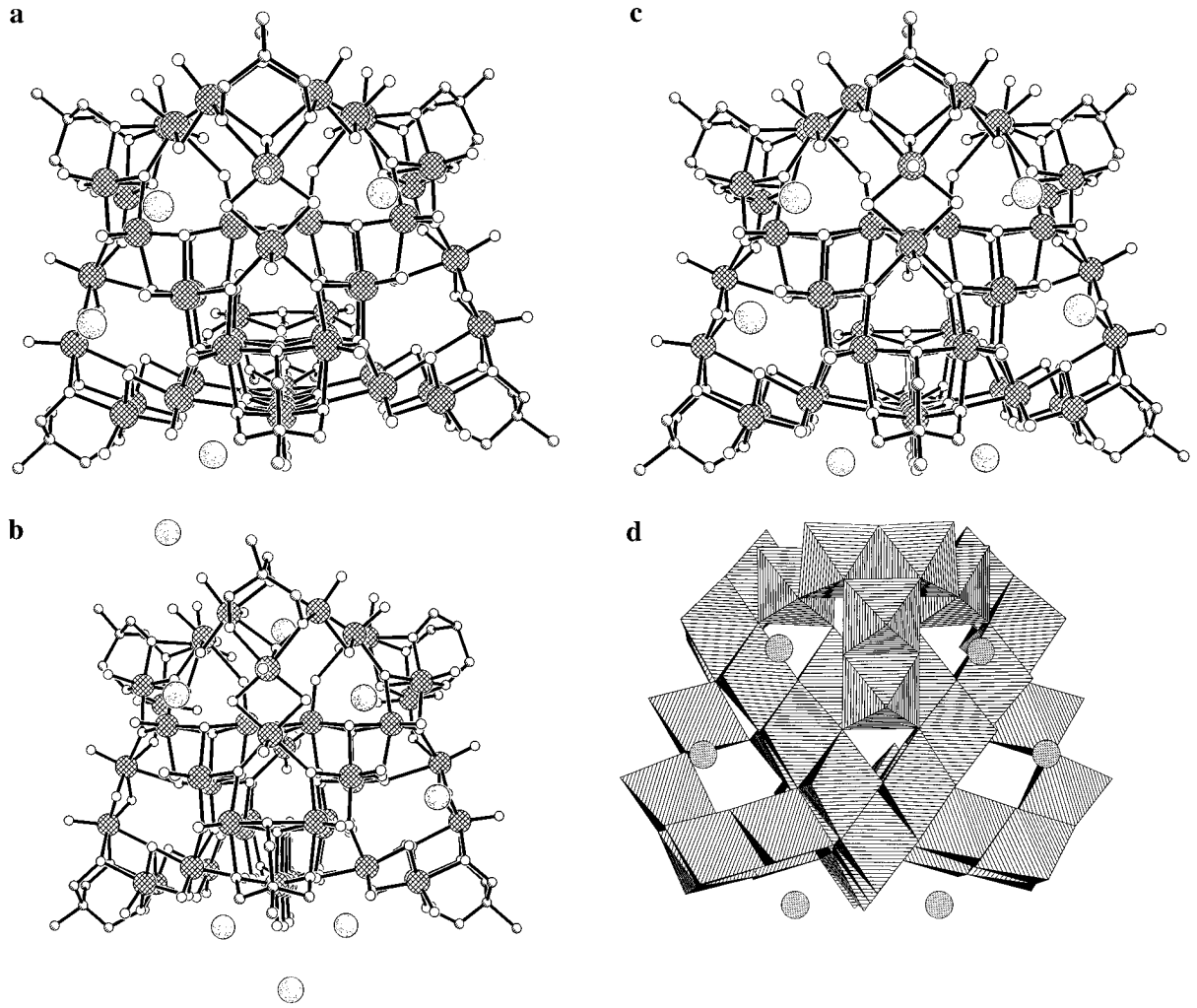

Figure 9. Illustration of the Na^+ occupancies of the cavities on the surfaces of the various clusters: (a) the four sites occupied for **3**; (b) the five sites occupied in **5** and the additional three loosely associated sites; (c) the full occupancy of six sites associated with **4** and **6**; (d) polyhedral view of the cluster surface and Na^+ positions, illustrating the construction of the minor cavities at the junction of two adjacent **3A** subunits, the central **3A′** subunit, and **3B** subunit, and the central ring **3C**.

The molybdenum−oxygen core of the anions of **3**, i.e. **3a**, consists of a $\{Mo_{42}O_{120}\}$ fragment, constructed from $\{MoO_6\}$ edge-sharing octahedra. Of the 120 oxygen atoms of this framework, 42 are terminal oxo groups with characteristic Mo−O distances in the 1.60−1.70 Å range and 21 are ligand alkoxy oxygen donors in the conventional doubly-bridging arrangement, with Mo−O distances of 2.08−2.22 Å. Of the remaining 67 oxo groups, 34 are triply-bridging between Mo sites, while 33 are doubly-bridging. The structure of **4** exhibits an identical distribution of major oxygen types to that listed for **3**, while **5** and **6** differ only in the substitution of the $\{MoO_3\}$ unit in the cavity for the $Na(H_2O)_3^+$ unit of **3** and **4**, with the concomitant change in classification of three $\{Mo_2O\}$ types of the latter to $\{Mo_3O\}$ types in **5** and **6**.

The doubly- and triply-bridging oxo groups of **3** and **4** may be further subclassified according to their metrical parameters. In this fashion, there are three major subclasses of doubly-bridging oxo groups: those with essentially symmetrical Mo−O distance in the range 1.91−1.98 Å, of which there are twenty-one; a set of six asymmetric $\{Mo_2O\}$ interactions with distinct Mo−O distances of *ca*. 1.85 and 2.00 Å, which are associated exclusively with the fusing of type **3A** subunits to **3B** fragments via the corner-sharing interaction of Mo(1b) and Mo(2c) metal sites; and a class of six highly asymmetric $\{Mo_2O\}$ interactions, exhibiting Mo−O distances of *ca*. 1.76 and 2.35 Å and associated with the linking of **3A** subunits to the **3C** central ring through the corner-sharing interaction of Mo(1b) and Mo(3) centers of the respective fragments. In view of this long Mo(1b)−oxo group distance, which contributes *ca*. 0.3 valence unit to the valence sum, the Mo(1b) sites are highly distorted octahedra, which may be alternatively described as square pyramidal sites with a weak axial interaction to the oxo group *trans* to the apical multiply-bonded oxide. The structures of **5** and **6** differ principally in utilizing three of the first subclass of oxo groups in linkage to the $\{MoO_3\}$ guest fragment, thus reducing the number of doubly-bridging $\{Mo_2O\}$ units to 30 and increasing the number of triply-bridging $\{Mo_3O\}$ units to 37.

There are two major subclasses of triply-bridging oxo groups encountered for **3** and **4** which are clearly distinguishable by their distinctive geometries. The first type of which there are 19 exhibit a pyramidal $\{Mo_3O\}$ unit (Figure 8a) with uniformly long Mo−O distances of *ca*. 2.25 Å. Valence sum calculations provide valences in the range 1.0−1.3 for these sites in the absence of protonation or close contacts to Na^+ cations, establishing such sites quite unambiguously as the protonation sites. The remaining 15 $\{Mo_3O\}$ sites shown in Figure 8b possess a planar Y-shaped $\{Mo_3O\}$ grouping with two Mo−O distances of *ca.* 2.0 Å and a third of 2.10 Å, which are consistent with a valence of *ca.* 2.0 for these sites. The structures of **5** and **6** exhibit a similar pattern of triply-bridging sites but with an additional three $\{Mo_3O\}$ unit contribution by the introduction

of the $\{MoO_3\}$ fragment into the cavity. The additional $\{Mo_3O\}$ groupings are of the latter Y-shaped class.

The bridging oxo groups may be further subdivided according to their role in linking the various subunits **3A**, **3B**, and **3C**, to provide the labeling scheme adopted for Figure 5 and Table 10. Thus, O(1d) types bridge the Mo(1b) site of **3A** with Mo(3) of the central ring **3C**, O(2d) types link Mo(1b) of the **3A** fragments to Mo(2c) of the **3B** subunits, and O(3d) bridges Mo(1a) and Mo(1b) sites within the same **3A** fragment.

The overall complexity of the fragment connectivity is manifested in the variety of triply-bridging oxo types. The O(1t) sites bridge the triangular arrays of alkoxide coordinated Mo(1a) and Mo(2a) and Mo(2c) sites of fragments **3A**, **3A′**, and **3B**. The O(2t) subclass links Mo(1a)′ and Mo(1b)′ sites of the **3A′** cluster to the Mo(1c) centers of the fragments **3A**. The Mo(2a) and Mo(2b) centers of the **3B** subunit are bridged and linked to the Mo(1b) sites of the **3A** fragment through O(3t) oxo types. The oxo groups classified as O(4t) types serve to link the Mo(1c) site of type **3A** clusters and each of the three Mo(1b)′ sites of **3A′** to two of the Mo(3) sites of the central **3C** ring. Molybdenum sites from three fragment types are linked through O(5t) types: each of the three Mo(1b)′ sites of **3A′** is connected to the Mo(2b) center of **3B** and a Mo(3) site of the ring **3C**. The O(6t) centers bridge adjacent Mo(3) sites of **3C** to the Mo(2b) center of **3B**. The O(7t) positions bridge adjacent Mo(3) sites of the **3C** fragment to the guest $\{MoO_3\}$ group in **5** and **6** and to the $Na(H_2O)_3^+$ grouping in **3** and **4**. The types and descriptions of oxygen atoms within the $\{XMo_{42}O_{130}\}$ cores of **3**−**6** are summarized in Table 10; the total numbers of the classes within the clusters are also listed.

The $\{Mo_{42}O_{130}\}$ cores of **3**−**6** are essentially identical, as suggested by the metrical parameters of Table 11. The anionic clusters of **3** and **4** envelop the $\{Na(H_2O)_3\}^+$ unit within the molecular cavity through interaction to the three O(7t) oxo groups of the central ring. In contrast, the clusters of **5** and **6** encapsulate a neutral $\{MoO_3\}$ moiety, once again *via* linkage to the O(7t) oxo donor set.

The clusters may be distinguished not only by the identity of the guest molecule but also by the number of Na^+ cations and protonation sites associated with the anionic clusters. As shown in Figure 9, in addition to the major molecular cavity which is occupied by $\{Na(H_2O)_3\}^+$ or $\{MoO_3\}$, the clusters possess six minor cavities or recesses on the convex surface of the cluster which have dimensions appropriate for the accommodation of Na^+ cations. In the structures of this study, four, five, or six of these sites are populated by Na^+ cations for **3**, **5** and **4**, and **6**, respectively. Invariably, each Na^+ cation is bonded to one O(5t) oxo group and two O(3d) oxo groups, one from each of two adjacent **3A** subunits. These minor cavities are thus formed by the cleft between adjacent **3A** subunits and the fusion of the central **3A′** subunit with ring **3C** and one **3B** subunit.

The structure of **5** is most unusual, in that one of these six sites is not occupied, but rather three additional locations on the exterior, linked to terminal oxo groups, and one unique site siting at the mouth of the major cavity (Figure 10). In this instance, not only has the cavity been occupied by the $\{MoO_3\}$ group but also the entrance has been "plugged" by the addition of the Na^+ cation.

The Na^+ cations also serve to link adjacent cluster anions into 1-D chains, which in turn are aligned so as to form layers of anions and inorganic cations. In the case of **3**, the central pairs of Na^+ cations, directly opposite the guest $Na(H_3O)_3^+$ groups, bridge pairs of clusters, as shown in Figure 11. The resultant cluster dimers are in turn linked through interaction

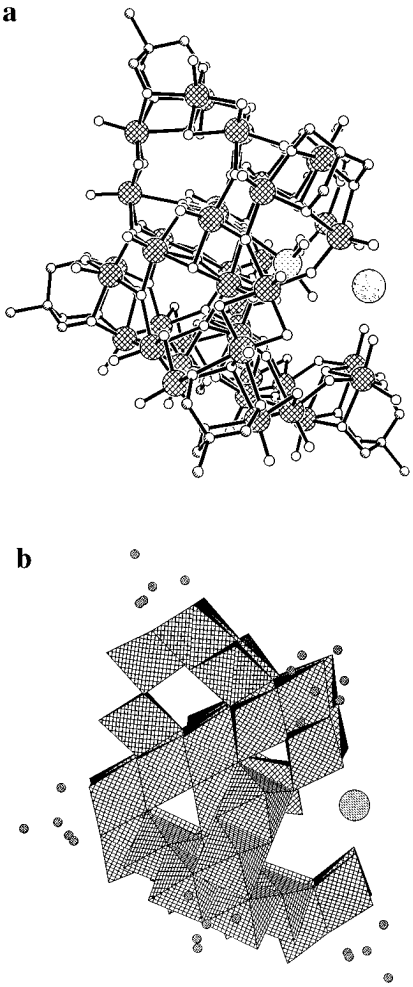

Figure 10. (a) View of the unusual Na^+ cation location in **5**, which serves to plug the mouth of the major cavity of the cluster. The $\{MoO_3\}$ guest and the Na^+ cation are displayed as large highlighted spheres for contrast. (b) Polyhedral representation, illustrating the position of the Na^+ cation with respect to the "pincers" of the grapple arms.

of one of the remaining Na^+ sites of each cluster with the pendant alcohol −OH groups of adjacent dimer pairs. The zigzag 1-D chains which are thus produced orient so as to form layers of anion clusters and Na^+ cations. Water molecules and organoammonium cations occupy the interlayer regions.

In the case of species **4** and **6** where all six minor cavities of the anion cluster are occupied, a different linkage pattern is adopted. As shown in Figure 12, rather than employing the central pair of Na^+ cations as in **3**, the peripheral pairs of Na^+ cation sites are used in bridging an anion cluster to two adjacent clusters. Once again, a puckered chain of Na^+-linked clusters is formed, and these chains in turn orient to produce layers of clusters and Na^+ cations.

Since anion **5** exhibits a vacancy at one of the six minor cavities available as Na^+ sites, the cation bridging of anion clusters is distinct from that adopted by **4** and **6**. A peripheral pair from each of two adjacent clusters serves to form a dimer of clusters in a fashion similar to that adopted at one site by **4** and **6**. However, these dimer units are then linked through exterior Na^+ cations into tetranuclear units. As shown in Figure 13, these tetranuclear units are linked into 1-chains which are two clusters in width, rather than one, the motif adopted by **3**, **4**, and **6**. The role of the Na^+ cations in bridging the cluster anions into 2-D networks of 1-D chains appears to be a crucial feature of the solid state organization of these materials. The isolation of crystalline phases of the superclusters exclusively for the Na^+ derivatives may reflect the unique charge, size, and

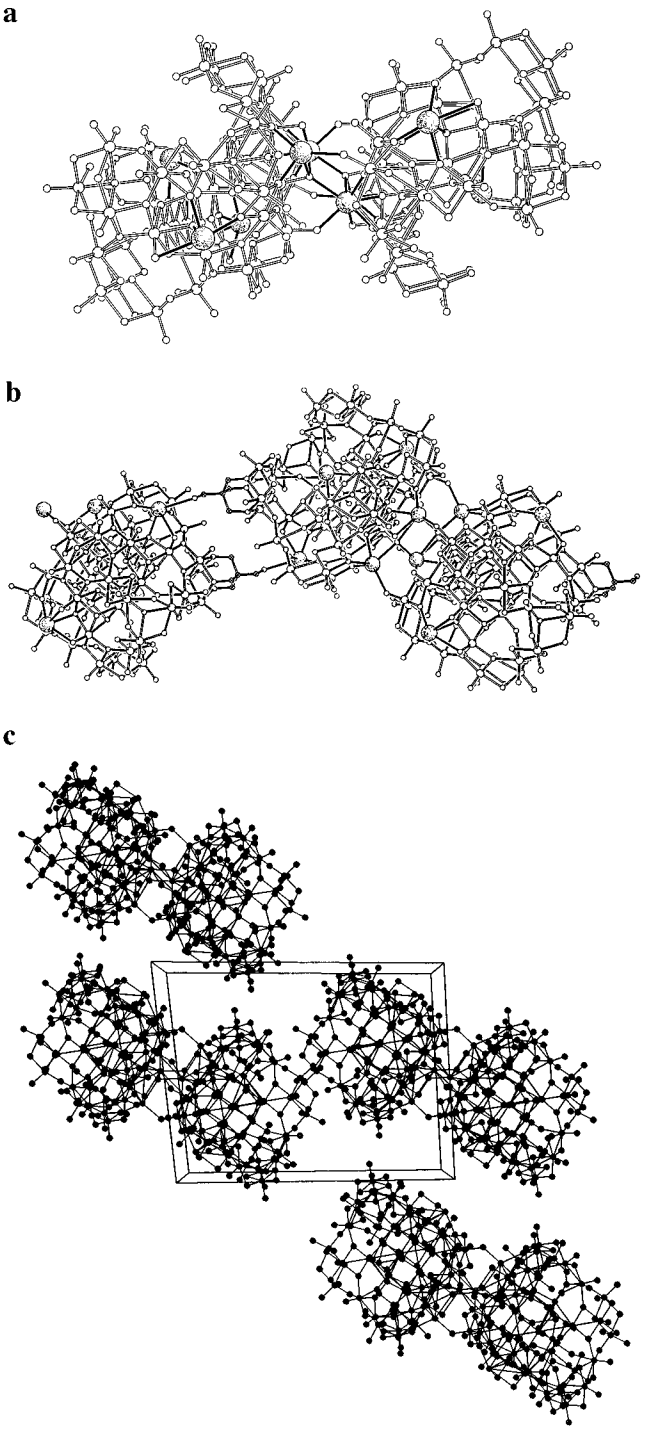

Figure 11. (a) Schematic view of the back-to-back linking of two adjacent anion clusters in **3**. (b) Bridging of one anion to two adjacent clusters, through the two types of interactions: back-to-back through two surface-bound Na^+ cations from each cluster and through bonding of Na^+ cations to pendant ligand $-OH$ groups. (c) Orientation of adjacent chains to produce layers of anion clusters and Na^+ cations.

coordination requirements of the Na^+ cation which render this group ideal for its structural role in the organization of the structures of the solid phases.

Valence sum calculations in the oxo groups of **3**−**6** unambiguously identify 19 triply bridging oxo groups as protonation sites or sites interacting with Na^+ cations. These oxo groups are exclusively of the types O(1t), O(5t), O(6t), and the subgroup of the O(4t) class bridging the **3A′** and **3C** subunits. Since different numbers of O(6t) sites are used in bonding to Na^+ cations in the different structures, there are different numbers of triply-bridging oxo groups protonated in the series: 15, 13, 14, and 13 sites for **3**−**6**, respectively. For structures **3** and **5**, the total number of protonation sites, Na^+ cations, and organic ammonium cations provides charge neutrality. In the cases of **4** and **6**, one and two additional cations, respectively, are required to achieve charge balance.

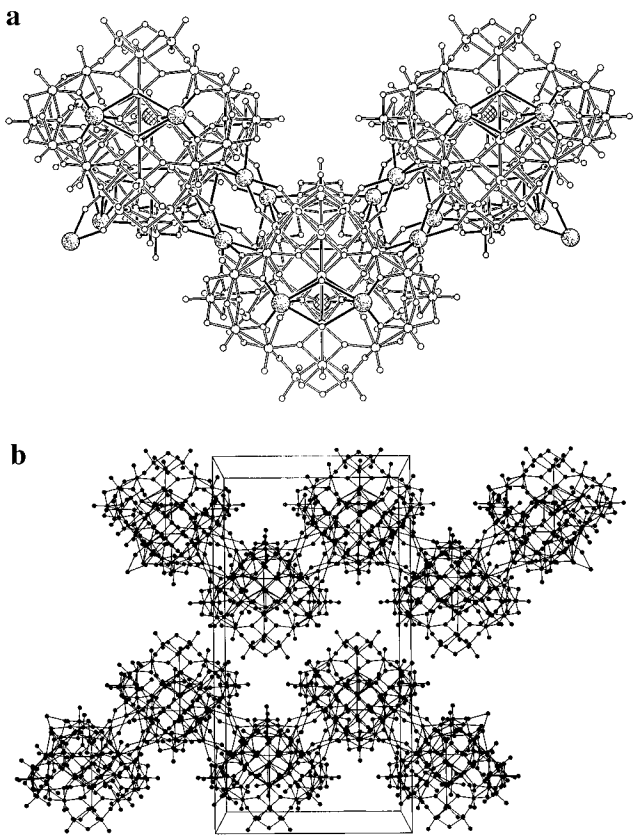

Figure 12. (a) Side-to-side linkage of clusters, adopted in **4** and **6**. (b) Orientation of adjacent chains in **6**.

For both **4** and **6**, there are doubly-bridging sites of the type O(3d) with somewhat long Mo−O distances which may participate in strong hydrogen bonding to a hydronium cation. In the structure of **4**, there is one unique pair of doubly-bridging oxo groups, O(29) and O(33), which bridge adjacent pairs of Mo(V) centers in one of the **3A** subunits. As shown in Figure 14, these exhibit close contacts of 2.35(1) and 2.43(1) Å, respectively, with O(150), which is assigned as a hydronium cation on the basis of these significant hydrogen-bonding interactions. It is instructive that all other doubly-bridging oxo groups of **4** exhibit significantly different structural properties. The oxo groups of classes O(1d) and O(2d) are of the asymmetrically bridging type with valence sums in the range 1.90−2.00 Å. The remaining O(3d) oxo groups either participate in bonding to Na^+ cations or form weak hydrogen-bonding interactions with the organic ammonium cations or the water molecules of crystallization, at distances of 2.75−2.85 Å. The short distances associated with O(29)−O(150) and O(33)−O(150) are unique to this pair.

Similar structural features are observed for **6**, with the exception that there are two such sites rather than one. Once again, O(3d) oxo types associated with adjacent pairs of Mo(V) centers of **3A** subunits are found to associate at *ca.* 2.40 Å with a suspected hydronium cation: in this case, the doubly-bridging oxo groups O(3) and O(20) with O(104). The symmetry of the cluster results in two equivalent sites of this type. Once again, all other doubly-bridging oxo groups exhibit unexceptional metrical parameters. It is instructive that the structures of **3** and **5**, which require no hydronium cations or

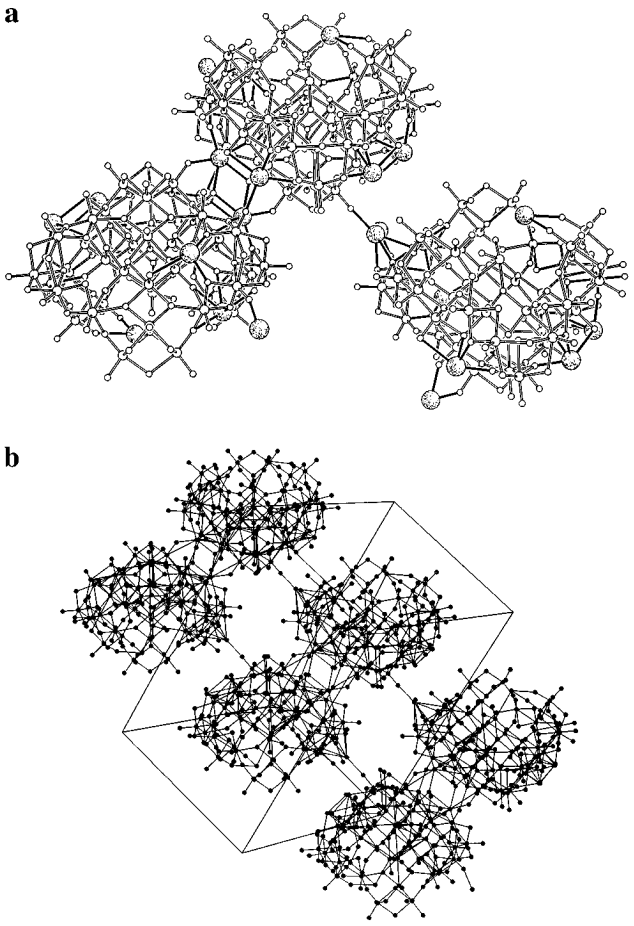

Figure 13. (a) Linking of anion clusters by Na^+ cations in **5** to produce chains two anion clusters in thickness, shown in (b).

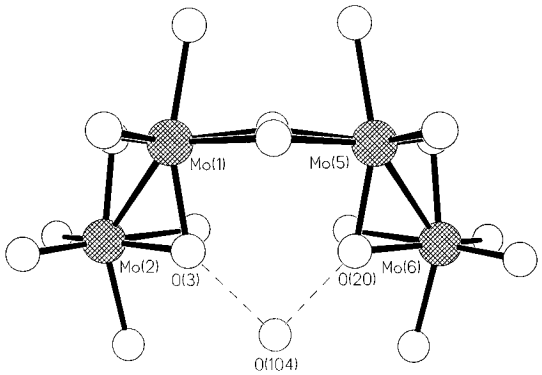

Figure 14. Possible hydronium cation site in the structure of **6**. There are two such sites for **6** and one for **4**. Structures **3** and **5** reveal no such close contacts.

further protonation of oxo groups for charge balance, reveal no oxo group−hydration sphere interactions with O···O distances less than 2.75 Å. While these structural arguments for the identities of the hydronium cations may not be totally conclusive, the metrical parameters associated with the oxo groups of the four structures **3**−**6** are consistent and indicative of the presence of hydronium cations at the proposed sites.

It is also noteworthy, as illustrated in Figure 15, that the $\{Mo_{16}O_{52}\}$ unit of **2** provides the structural core for the construction of the anionic frameworks of **5** and **6**. In this fashion, the structure of the anionic clusters $[(MoO_3)H_n Mo_{42}O_{109}\{(OCH_2)_3CR\}_7]^{(23-n)-}$ may be derived formally from the $\{Mo_{16}O_{52}\}$ unit by condensing a $\{(CH_2)_3CR\}^{3+}$ grouping on one triangular face of the $\{Mo_{16}O_{52}\}$ cage, linking three of the four $\{MoO_3\}$ trioxomolybdate units of this core with

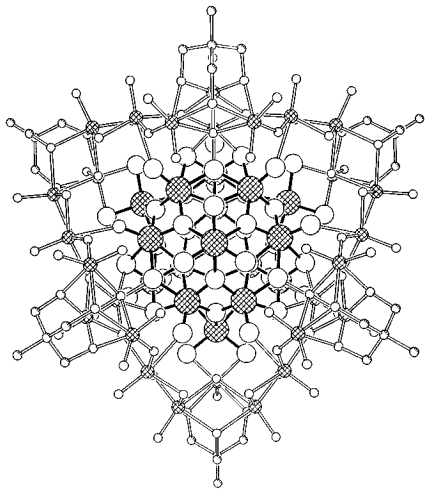

Figure 15. View of the structure of the $[(MoO_3)H_n Mo_{42}O_{109}\{(OCH_2)_3CR\}_7]^{(23-n)-}$ cluster of **5** and **6**, highlighting the $\{Mo_{16}O_{52}\}$ core.

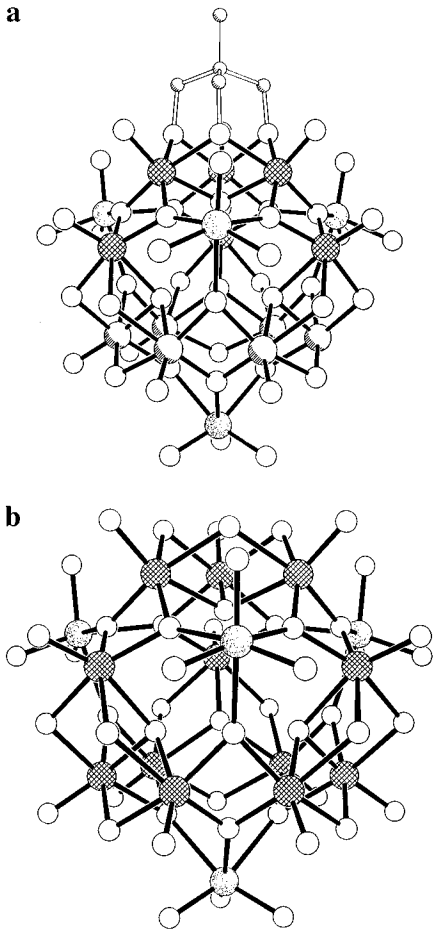

Figure 16. (a) The $\{Mo_{16}O_{49}[(OCH_2)_3CR]\}$ unit of **5** and **6**, whose molybdenum−oxide core is structurally related to the $\{Mo_{16}O_{52}\}$ unit of **1** and **2**. The six Mo(3) sites of the central **3C** ring are highlighted on the bottom left of the spheres; the six Mo(1a)′ and Mo(1b)′ centers of the unique **3A′** subunits are displayed as cross-hatched spheres; and the three Mo(1c) centers, one from each of the three **3A** subunits, and the unique guest site are represented by the heavily highlighted spheres. (b) The $\{Mo_{16}O_{52}\}$ core of **1** and **2** in the appropriate orientation for comparison with (a).

$\{Mo_5O_{14}[(OCH_2)_3CR]\}$ fragments, and connecting the central ring of the $\{Mo_{16}O_{52}\}$ unit and these latter fragments through three **3B** type subunits. As shown in Figure 16, the $\{Mo_{16}O_{52}\}$ central core of the superclusters is constructed from the central

ring **3C**, the unique **3A′** subunit, three Mo(1c) centers, one from each of the three **3A** subunits, and the guest $\{MoO_3\}$ group.

A curious feature of the $\{Mo_{16}O_{52}\}$ unit is the apparent ability to accommodate variable numbers of protons within the central cavity. Thus, charge considerations for the anion of **2** suggest that two protons occupy the cavity, while for **5** and **6**, the metrical parameters and charge considerations are consistent with four protonation sites within the cavity. However, it should be noted that formal molybdenum oxidation state distributions of the cores are quite distinctive: $\{Mo^{VI}_4Mo^{V}_{12}O_{52}\}$ in **2** and $\{Mo^{VI}Mo^{V}_{15}O_{52}\}$ in **5** and **6**, as suggested by valence bond arguments.[51]

While it is tempting to speculate that the $\{Mo_{16}O_{52}\}$ core may mediate template-directed syntheses of more complex clusters from simple soluble precursors or clusters of the type found in **3**−**6** but incorporating a range of substrate fragments, attempts to vary the identity of the guest molecule or to isolate other cluster types have proved fruitless. However, the presence of Na^+ cations is required for the isolation of **3**−**6**, suggesting that these may serve to direct the organization of the various structural subunits of the superclusters, as well as to balance charge. The interplay of cation radii and charge-compensating effects appears to play a dominant role in limiting the choice of cationic template. However, the dimensions of the minor clefts associated with the convex surface of the clusters, as well as those of the major cavity, are compatible with the incorporation of a number of transition metal cations. Likewise, the $[M_3O_4\{(OCH_2)_3CR\}]$ grouping may be extended to V(VI) and V(V), and possibly W(V), as well as molybdenum, suggesting that mixed-metal clusters based on the prototypes of this study may be accessible.

Magnetic Properties. The temperature-dependent magnetic data for **5** show a magnetic transition to a weakly ferromagnetic state at a temperature of about 55 K. At high temperatures ($T > 100$ K), the susceptibility data exhibit Curie−Weiss paramagnetism. The high-temperature magnetic data were fitted to the Curie−Weiss law:

$$\chi = X/(T - \Theta) = N\gamma^2\mu_B{}^2S(S+1)/[3\kappa(T-\Theta)] \quad (1)$$

The data are plotted in Figure 17 as the temperature dependent molar magnetic susceptibility with the inverse magnetic susceptibility of the material plotted in the insert. The resulting least-squares-fitted parameters are $C = 0.278$ emu K mol^{-1} and

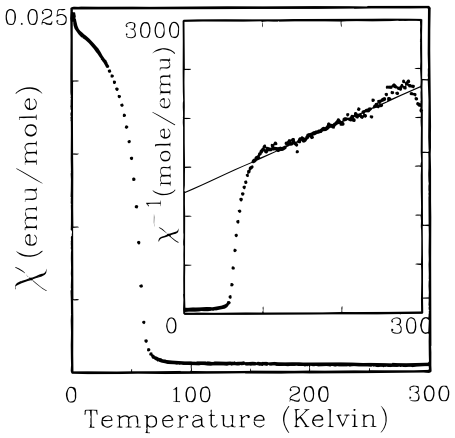

Figure 17. Magnetic susceptibility of **5** plotted as a function of temperature over the 1.7−300 K temperature region. The inset shows the inverse magnetic susceptibility plotted as a function of temperature. The line drawn through the data is the fit to the Curie−Weiss model as described in the text.

$\Theta = -340$ K. The large negative Θ corresponds to a strong antiferromagnetic coupling between the unpaired electrons which give rise to the weak ferromagnetic transition at lower temperatures. The cluster contains a mixture of paramagnetic and diamagnetic molybdenum centers; however the magnetic data indicate that most of the magnetism has been quenched at room temperature and the residual magnetism that remains is what is measured between 1.7 and 300 K as shown in Figure 17. The magnitude of the magnetic susceptibility data corresponds to an average of approximately one unpaired electron per cluster. The residual paramagnetism undergoes a weak ferromagnetic ordering at $T_c = 50$ K.

Acknowledgment. This work was supported by NSF Grant CHE-9318824 to J.Z. C.J.O. acknowledges support from the Louisiana Education Quality Support Fund [LESQF, (RF/1994−94)-ENH-TR-60), administered by the Regents of the State of Louisiana.

Supporting Information Available: Tables of non-hydrogen positional parameters, bond lengths, bond angles, and anisotropic thermal parameters for **1**−**6** and tables of hydrogen positional parameters for **3**, **4**, and **6** (108 pages). Ordering information is given on any current masthead page.

IC9508841